

Comments on Baryons in Holographic QCD

Shigenori Seki* and Jacob Sonnenschein†

*The Raymond and Beverly Sackler School of Physics and Astronomy
Faculty of Exact Sciences, Tel Aviv University, Ramat Aviv 69978, Israel*

Abstract

We generalize the description of baryons as instantons of Sakai-Sugimoto model to the case where the flavor branes are non-anti-podal. The later corresponds to quarks with a “string endpoint mass”. We show that the baryon vertex is located on the flavor branes and hence the generalized baryons also associate with instantons. We calculate the baryon mass spectra, the isoscalar and axial mean square radii, the isoscalar and isovector magnetic moments and the axial coupling as a function of the mass scale M_{KK} and the location ζ of the tip of U-shaped flavor D8-branes. We determine the values of M_{KK} and ζ from a best fit comparison with the experimental data. The later comes out to be in a forbidden region, which may indicate that the incorporation of baryons in Sakai-Sugimoto model has to be modified. We discuss the analogous baryons in a non-critical gravity model. A brief comment on the single flavor case ($N_f = 1$) is also made.

9 October 2008

* sekish@post.tau.ac.il

† cobis@post.tau.ac.il

1. Introduction

Baryons were incorporated into the $AdS_5 \times S^5$ model in [1,2] via a D5-brane wrapping the S^5 with N_c strings attached to it and ending up at the boundary. The strings are needed to cancel an N_c charge in the world-volume of the wrapped brane that follows from the RR flux of the background. This object which is the dual of an external baryon, namely with infinitely heavy quarks was further discussed in [3–5] and was generalized also to confining backgrounds [6] where it was found that their energy was linear in N_c and in the “size” of the baryon on the boundary.

A realization of a dynamical baryon has become possible once flavor probe branes were added to holographic models. A prototype of such a model is Sakai-Sugimoto (SS) model [7]. This model is based on placing a stack of N_f probe D8-branes and a stack of N_f probe anti-D8-branes connected in a U-shaped cigar profile, into the model of [8] of near extremal D4-branes. The baryon vertex is immersed in the probe brane at the tip of the cigar. In [9] it was shown that the baryon corresponds to an instanton of the five-dimensional effective $U(N_f = 2)$ gauge theory. The physical properties of this baryon were analyzed in several papers [10–25]¹. These include in particular the mass, size, mass splitting, the mean square radii, magnetic moments, various couplings and more. A comparison with experimental data reveals an agreement similar, or even better, than the one found in the Skyrme model [28]. In spite of this success the baryons of the model of [9] suffer from several problems. The size of the baryon is proportional to $\lambda^{-1/2}$ where λ is the four-dimensional 't Hooft parameter. Since the gravitational holographic model is valid only in the large λ limit, this implies that stringy corrections have to be taken into account. Another drawback of the model is that the scale of the system associated with the baryonic structure is roughly half the one needed to fit to the mesonic data².

SS model has a generalization [30], where the location of the probe branes in the compactified direction is not anti-podal, or differently stating the tip of the probe brane is at a radial location $u_0 > u_{KK}$ where u_{KK} is the minimal value of the radial direction of the background. The difference between the two cases is drawn in fig. 1.

¹ The different approach for the baryons in SS model has been studied by [26,27].

² Ref. [29] has shown that this problem is substantially improved in the AdS/QCD model.

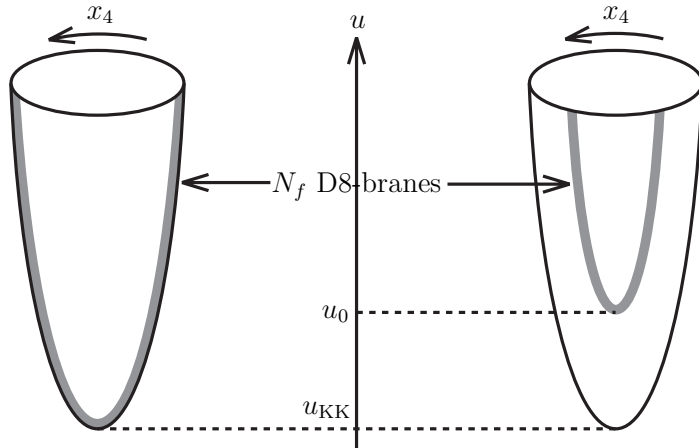


fig. 1 The probe D8-branes in the cigar background

The non-anti-podal case is in fact a family of models characterized by the separation distance L or a “string endpoint mass” of the quark [31]³. A natural question to ask is how do the properties of the baryon depend on the additional parameter and in particular whether the problems mentioned above in the context of the anti-podal case can be circumvented. This is the main goal of this paper. As a first step we address the question of where the baryon vertex is located in the generalized setup. We show that in the confining phase it is again immersed in the probe brane. In the deconfining phase above a certain critical temperature, the baryon vertex falls into the “black hole” and thus the baryon is dissolved. The main part of this paper includes a repetition of the calculations performed in [9,37] of the properties of the baryons now made in the generalized setup with non-trivial stringy mass namely a non-anti-podal configuration. The expressions for the mass spectra, mean radii, magnetic moments and couplings are derived as a function of the scale and the parameter which measures the deviation from the anti-podal configuration. It has turned out that the generalized setup does not resolve the problem of the size of the baryon. We have found that the data can be fit with the same scale that governs the mesonic spectra provided the location of the probe brane is in an unphysical location “below the tip of the cigar”. It seems to us that this is an indication of a problem of the baryonic setup of SS model.

We also analyze the baryons of the non-critical model [38] based on the incorporation of N_f probe D4-branes into the background of a near extremal D4-branes residing in six dimensions. It is shown that the problem of the small size of the baryon is avoided in this

³ For attempts to introduce the QCD or current algebra mass, see [32–36].

model. We also setup the stage for the open problem of the baryons of a single flavor brane namely $N_f = 1$.

The paper is organized as follows. After this introduction we describe the general setup of the non-anti-podal SS model. In Section 3 we analyze the baryonic configuration in the generalized setup and determine that the location of the baryon vertex is on the flavor brane. Section 4 is devoted to a detailed analysis of the baryon properties following [9,37] in the non-anti-podal geometry. The values of the scale and the location of the flavor brane that fit the data in an optimal way are determined. We then present the open question of the baryon for a single flavor case. Section 6 presents an analysis similar to the one in Section 4 but in the context of a non-critical six-dimensional model. We end with a short summary, list of conclusions and open questions. Appendix includes the computations of the location of the baryon vertex in the general case of Dp -brane background with $D(8-p)$ -branes wrapping an S^{8-p} cycle.

2. The general setup of the non-anti-podal Sakai-Sugimoto model

SS model [7] is a system which consists of N_c coincident color D4-branes and N_f coincident flavor D8-branes. When N_c is large, the D4-branes are regarded as the background, of which metric is given by

$$\begin{aligned}
 ds^2 &= \left(\frac{u}{R}\right)^{\frac{3}{2}} \left[\eta_{\mu\nu} dx^\mu dx^\nu + f(u) dx_4^2 \right] + \left(\frac{R}{u}\right)^{\frac{3}{2}} \left[\frac{du^2}{f(u)} + u^2 d\Omega_4^2 \right], \\
 e^\phi &= g_s \left(\frac{u}{R}\right)^{\frac{3}{4}}, \quad F_{(4)} = \frac{2\pi N_c}{V_4} \epsilon_4, \quad R^3 := \pi g_s N_c l_s^3, \quad f(u) := 1 - \left(\frac{u_{\text{KK}}}{u}\right)^3,
 \end{aligned}
 \tag{2.1}$$

where $\eta_{\mu\nu} = \text{diag}(-1, 1, 1, 1)$. The volume of unit four sphere V_4 is equal to $8\pi^2/3$. The x_4 direction is compactified by the circle with the period

$$\delta x_4 = \frac{4\pi R^{\frac{3}{2}}}{3u_{\text{KK}}^{\frac{1}{2}}}.
 \tag{2.2}$$

This period is determined so that the singularity at the tip $u = u_{\text{KK}}$ is excluded. Then the Kaluza-Klein mass scale M_{KK} becomes

$$M_{\text{KK}} := \frac{2\pi}{\delta x_4} = \frac{3u_{\text{KK}}^{\frac{1}{2}}}{2R^{\frac{3}{2}}}.
 \tag{2.3}$$

The flavor D8-branes are realized as the probe in the D4-branes' background (2.1). The action of the coincident D8-branes consists of the two parts,

$$S_{\text{D8}} = S_{\text{DBI}} + S_{\text{CS}}. \quad (2.4)$$

S_{DBI} is the Dirac-Born-Infeld (DBI) action,

$$S_{\text{DBI}} = T_8 \int d^9x e^{-\phi} \sqrt{-\det(g_{MN} + 2\pi\alpha' \mathcal{F}_{MN})}, \quad (2.5)$$

where the D8-brane's tension is denoted by $T_8 = (2\pi)^{-8} l_s^{-9}$. The induced metric g_{MN} is computed from (2.1),

$$ds_{\text{D8}}^2 = \left(\frac{u}{R}\right)^{\frac{3}{2}} \eta_{\mu\nu} dx^\mu dx^\nu + \left[\left(\frac{u}{R}\right)^{\frac{3}{2}} f(u) + \left(\frac{R}{u}\right)^{\frac{3}{2}} \frac{u'^2}{f(u)} \right] dx_4^2 + \left(\frac{R}{u}\right)^{\frac{3}{2}} u^2 d\Omega_4^2, \quad (2.6)$$

where u' denotes du/dx_4 . \mathcal{F} is a $U(N_f)$ gauge field strength on the worldvolume of the D8-branes. The $U(N_f)$ gauge field \mathcal{A} has also Chern-Simon action S_{CS} ,

$$S_{\text{CS}} = \frac{N_c}{24\pi^2} \int \text{tr} \left(\mathcal{A} \mathcal{F}^2 - \frac{i}{2} \mathcal{A}^3 \mathcal{F} - \frac{1}{10} \mathcal{A}^5 \right). \quad (2.7)$$

where the integral is now a five-dimensional one.

We shall study the shape of the D8-branes by the analyses of the classical solution of (2.4) without the gauge fields. In terms of (2.6), the DBI action (2.5) is written down

$$S_{\text{DBI}} = \frac{T_8 \Omega_4}{g_s} \int d^4x dx_4 u^4 \sqrt{f(u) + \left(\frac{R}{u}\right)^3 \frac{u'^2}{f(u)}} =: S_0[u(x_4)]. \quad (2.8)$$

Since the Hamiltonian calculated from this action is the function of only u , we can put the Hamiltonian constraint,

$$\frac{u^4 f(u)}{\sqrt{f(u) + \left(\frac{R}{u}\right)^3 \frac{u'^2}{f(u)}}} = \text{constant} = u_0^4 \sqrt{f(u_0)}, \quad (2.9)$$

where we used $u(0) = u_0$ and $u'(0) = 0$. Note that $u_0 \geq u_{\text{KK}}$. The Hamiltonian constraint is rewritten as

$$\frac{du}{dx_4} = \pm \left(\frac{u}{R}\right)^{\frac{3}{2}} f(u) \sqrt{\frac{u^8 f(u)}{u_0^8 f(u_0)} - 1}. \quad (2.10)$$

The solution of this equation implies that the D8-branes are U-shape in the cigar geometry expanded by the (u, x_4) coordinates (see also fig. 1). The boundary value $x_4(u = \infty) := L/2$ is evaluated from (2.10)

$$L = \int_{-L/2}^{L/2} dx_4 = 2 \int_{u_0}^{\infty} \frac{du}{|u'|} = 2 \int_{u_0}^{\infty} \left(\frac{R}{u}\right)^{\frac{3}{2}} \frac{1}{f(u) \sqrt{\frac{u^8 f(u)}{u_0^8 f(u_0)} - 1}} du. \quad (2.11)$$

L denotes the separation along the x_4 direction between the D8-branes at $u = \infty$. The equation (2.11) relates the parameter u_0 at the IR ($u = u_0$) with L at the UV ($u = \infty$). When u_0 is equal to u_{KK} , in other words, $L = \delta x_4/2$, the D8-branes are located at the anti-podal positions on the circular x_4 direction. This anti-podal case is the original SS model [7,39].

3. The baryon configuration in the generalized Sakai-Sugimoto model

The external baryon of the model of [1] was explored in [6]. It is composed from a baryon vertex which is a D4-brane wrapped on S^4 and N_c fundamental strings stretched between this D4-brane and the boundary. A dynamical baryon in the model of [7] differs from the external one in that the strings end on the probe flavor D8-branes and not on the boundary. The leading order action, which is the sum of the action of the D4-brane and the action of the N_c strings, takes the form

$$S = -T_4 \int dt d\Omega_4 e^{-\phi} \sqrt{-\det g_{\text{D4}}} - N_c T_f \int dt du \sqrt{-\det g_{\text{string}}} =: - \int dt E.$$

where E is the energy density and

$$T_4 = (2\pi)^{-4} l_s^{-5}, \quad T_f = (2\pi)^{-1} l_s^{-2}.$$

In a similar way one can consider the baryonic D $(8-p)$ -brane wrapped on the $(8-p)$ -dimensional sphere in the N_c D p -branes' background. This baryonic D-brane is regarded as the baryon vertex in the p -dimensional QCD-like theory. This analysis is presented in Appendix A.

The idea now is to find the location of the baryon vertex from the requirement of minimizing the energy. The energy as a function of the location of the baryon vertex will be calculated for the two distinct systems of the confining background and the deconfining one.

3.1. Confinement phase

The confining background is given by (2.1). Substituting this into the expression of the energy, we find

$$E(u_B; u_0) = \frac{N_c}{2\pi l_s^2} \left[\frac{1}{3} u_B + \int_{u_B}^{u_0} du \frac{1}{\sqrt{f(u)}} \right] =: \frac{N_c u_{\text{KK}}}{2\pi l_s^2} \mathcal{E}_{\text{conf}}(x; x_0),$$

$$\mathcal{E}_{\text{conf}}(x; x_0) = \frac{1}{3} x + \int_x^{x_0} \frac{dy}{\sqrt{1-y^{-3}}},$$

where $x := u_B/u_{\text{KK}}$ and $x_0 := u_0/u_{\text{KK}}$, the valid range of x is $1 \leq x \leq x_0$ (see fig. 2).

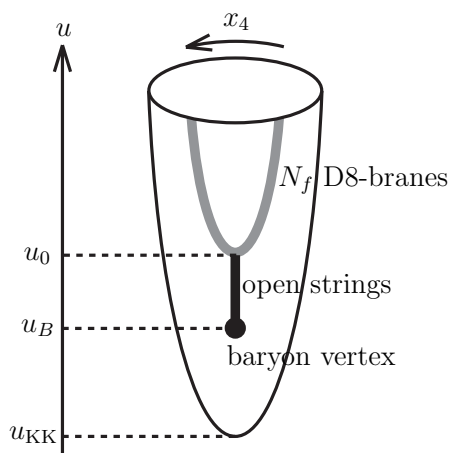


fig. 2 The baryon vertex in the confinement phase

Since $\mathcal{E}_{\text{conf}}(x; x_0)$ is a monotonically decreasing function of x , the energy E becomes minimum at $x = x_0$.

The meaning of this result is that like the anti-podal case also for the generalized case where $x_0 (= u_0/u_{\text{KK}}) \neq 1$ the baryon vertex is immersed inside the flavor probe branes. As was mentioned this is only a leading order calculation. It can be improved by adding the energy associated with the deformation of the wrapped brane due to the strings [40], and by relaxing the assumption that the strings stretch only along the radial direction. We believe that these improvements would not change the conclusion that the baryon vertex is located on the probe branes.

3.2. Deconfinement phase

Next we study the location of the baryon vertex in the deconfining phase. The difference in the background metric is that now the thermal factor is dressing the compactified

Euclidean time direction, and we replace the scale with the one related to the temperature u_T . Since the background metric in this phase reads

$$ds^2 = \left(\frac{u}{R}\right)^{\frac{3}{2}} [f_T(u)dt^2 + \delta_{ij}dx^i dx^j + dx_4^2] + \left(\frac{R}{u}\right)^{\frac{3}{2}} \left[\frac{du^2}{f_T(u)} + u^2 d\Omega_4^2\right],$$

$$f_T(u) := 1 - \left(\frac{u_T}{u}\right)^3,$$

the corresponding energy can be evaluated

$$E(u_B; u_0) = \frac{N_c}{2\pi l_s^2} \left[\frac{1}{3} u_B \sqrt{f_T(u_B)} + (u_0 - u_B) \right] =: \frac{N_c u_T}{2\pi l_s^2} \mathcal{E}_{\text{deconf}}(x; x_0),$$

$$\mathcal{E}_{\text{deconf}}(x; x_0) = \frac{1}{3} x \sqrt{1 - \frac{1}{x^3}} + (x_0 - x),$$

where $x := u_B/u_T$, $x_0 := u_0/u_T$ and $1 \leq x \leq x_0$.

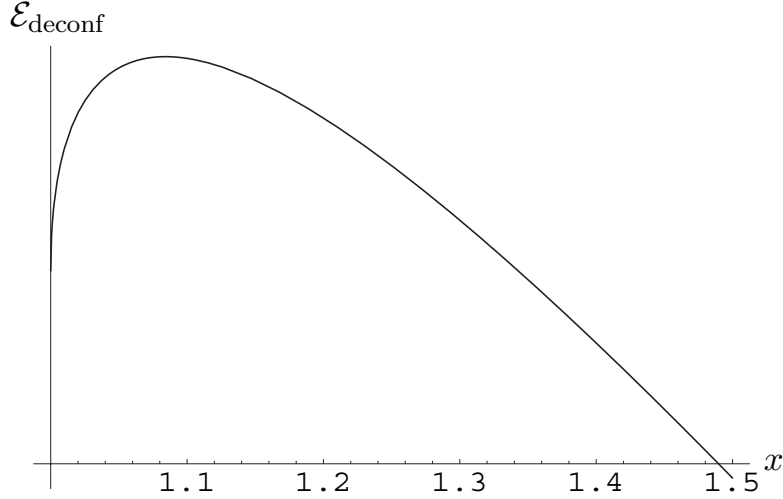


fig. 3 $\mathcal{E}_{\text{deconf}}(x)$

The energy (fig. 3) has a maximum at

$$x = \left(\frac{5 + 3\sqrt{3}}{8}\right)^{\frac{1}{3}} =: x_{\text{max}}.$$

x_{max} is approximately equal to 1.08422. We are also interested in the critical value x_{cr} which satisfies

$$E(1; x_0) = E(x_{\text{cr}}; x_0).$$

x_{cr} can be analytically calculated,

$$x_{\text{cr}} = \frac{5 + \sqrt{33}}{8} \approx 1.34307. \quad (3.1)$$

If $x_0 > x_{\text{cr}}$, then the energy becomes minimum at $x = x_0$ and the baryon vertex can exist at the tip of the U-shaped flavor D8-brane (fig. 4(a)). On the other hand, if $x_0 < x_{\text{cr}}$, then the energy becomes minimum at $x = 1$, that is to say, the baryon vertex falls down into the black hole (fig. 4(b)).

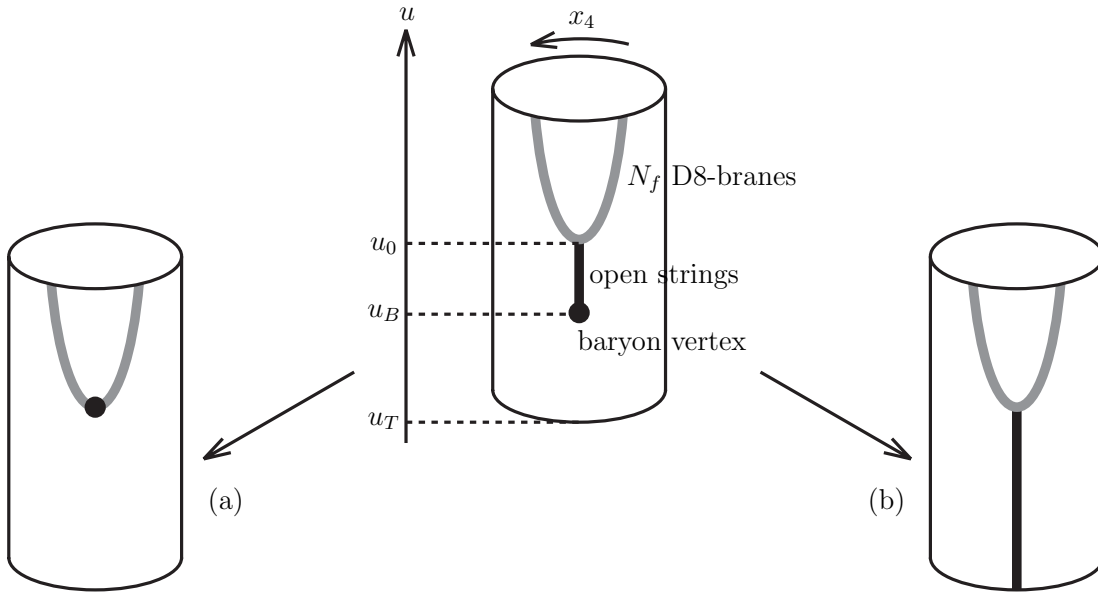


fig. 4 The baryon vertex in the deconfinement phase

The physical meaning of the picture is that for temperatures lower than a critical temperature, which is higher than the temperature of the confinement/deconfinement phase transition, the baryon vertex will be in the flavor brane just as in the zero temperature case. However, for higher temperature the baryon is dissolved via falling into the black hole and becoming N_c deconfined quarks.

4. Baryons as instantons in non-anti-podal Sakai-Sugimoto model

Once we found that the baryon vertex is immersed inside the probe flavor branes, to extract the properties of the baryons we have to repeat the computations done in [9,37] in the setup described in Section 2 rather than in the anti-podal geometry.

We turn on the $U(N_f)$ gauge fields as the perturbation around the classical solution $\mathcal{A} = 0$ discussed in Section 2. The DBI action (2.5) is expanded with respect to the gauge field,

$$S_{\text{DBI}} = S_0 + S_{\text{YM}} + \mathcal{O}(\mathcal{F}^3).$$

In a similar way to the anti-podal case it is convenient to introduce a new coordinate z defined by⁴

$$u = u_{\text{KK}}(\zeta^3 + \zeta z^2)^{\frac{1}{3}}, \quad \zeta = \frac{u_0}{u_{\text{KK}}}. \quad (4.1)$$

z and ζ are dimensionless. ζ takes a value in $[1, \infty)$ because of $u_0 \geq u_{\text{KK}}$, while z takes a value in $(-\infty, \infty)$. Though (2.10) implies that $x_4(u)$ is a double-valued function, the z coordinate makes it single-valued. The Yang-Mills part S_{YM} is calculated in terms of (2.6) and (4.1),

$$S_{\text{YM}} = -\kappa \int d^4x dz \text{Tr} \left[\frac{1}{2} h(z; \zeta) \mathcal{F}_{\mu\nu}^2 + M_{\text{KK}}^2 k(z; \zeta) \mathcal{F}_{\mu z}^2 \right], \quad (4.2)$$

where

$$h(z; \zeta) = \sqrt{\frac{\zeta^2 z^2 (\zeta^3 + \zeta z^2)}{(\zeta^3 + \zeta z^2)^{\frac{8}{3}} - (\zeta^3 + \zeta z^2)^{\frac{5}{3}} - \zeta^8 + \zeta^5}},$$

$$k(z; \zeta) = (\zeta^3 + \zeta z^2)^{\frac{1}{6}} \sqrt{\frac{(\zeta^3 + \zeta z^2)^{\frac{8}{3}} - (\zeta^3 + \zeta z^2)^{\frac{5}{3}} - \zeta^8 + \zeta^5}{\zeta^2 z^2}}$$

and $\kappa := \lambda N_c / (216\pi^3)$. λ is t'Hooft coupling, $\lambda := g_{\text{YM}}^2 N_c$. It is easy to check that for $\zeta = 1$ the anti-podal case is reproduced, namely, $h(z) = (1 + z^2)^{-1/3}$ and $k(z) = 1 + z^2$.

From now on, we use the $M_{\text{KK}} = 1$ unit. When necessary later, we shall be able to easily recover the factor M_{KK} . For the later convenience, we rescale the coordinate z and the field \mathcal{A}_z ,

$$\tilde{z} := \sqrt{\frac{h_0}{k_0}} z, \quad \mathcal{A}_{\tilde{z}} := \sqrt{\frac{k_0}{h_0}} \mathcal{A}_z. \quad (4.3)$$

h_0 and k_0 are defined through the expansions $h(z; \zeta) = h_0(\zeta) + \mathcal{O}(z^2)$ and $k(z; \zeta) = k_0(\zeta) + \mathcal{O}(z^2)$ respectively,

$$h_0 = \zeta \sqrt{\frac{3}{8\zeta^3 - 5}}, \quad k_0 = \zeta \sqrt{\frac{8\zeta^3 - 5}{3}}. \quad (4.4)$$

⁴ The ζ parameter is a measure of the ‘‘string endpoint mass’’ of the quark. The latter is defined as

$$m_q^s = \frac{1}{2\pi\alpha'} \int_{u_{\text{KK}}}^{u_0} du \sqrt{g_{00} g_{uu}}.$$

This quantity is neither the QCD mass nor the constituent mass of the quark. In a crude way a non-spinning meson has a mass of the form $M = T_{\text{st}} L + 2m_q^s$ (for equal endpoints).

It is clear from these expressions that there is a critical value of ζ , that is $\zeta_{cr} = (5/8)^{1/3} (< 1)$, such that necessarily $\zeta > \zeta_{cr}$. Recall however that by its definition $\zeta \geq 1$. We will come back to this point at the end of this section.

The action (4.2) is rewritten as

$$S_{\text{YM}} = -\tilde{\kappa}(\zeta) \int d^4x d\tilde{z} \text{Tr} \left[\frac{1}{2} \tilde{h}(\tilde{z}; \zeta) \mathcal{F}_{\mu\nu}^2 + \tilde{k}(\tilde{z}; \zeta) \mathcal{F}_{\mu\tilde{z}}^2 \right], \quad (4.5)$$

where $\tilde{h}(\tilde{z}; \zeta)$ and $\tilde{k}(\tilde{z}; \zeta)$ are defined in terms of (4.3) and (4.4) by

$$\tilde{h}(\tilde{z}; \zeta) := \frac{h(z; \zeta)}{h_0(\zeta)}, \quad \tilde{k}(\tilde{z}; \zeta) := \frac{k(z; \zeta)}{k_0(\zeta)}, \quad \tilde{\kappa}(\zeta) := \kappa \sqrt{h_0(\zeta) k_0(\zeta)} = \kappa \zeta. \quad (4.6)$$

Since $\tilde{h}(0; \zeta) = \tilde{k}(0; \zeta) = 1$, $\tilde{h}(\tilde{z}, \zeta)$ and $\tilde{k}(\tilde{z}, \zeta)$ can be expanded with respect to \tilde{z} as

$$\tilde{h}(\tilde{z}; \zeta) = 1 + \sum_{n=1}^{\infty} \tilde{h}_n(\zeta) \tilde{z}^{2n}, \quad \tilde{k}(\tilde{z}; \zeta) = 1 + \sum_{n=1}^{\infty} \tilde{k}_n(\zeta) \tilde{z}^{2n}. \quad (4.7)$$

For example, $\tilde{h}_1(\zeta)$ and $\tilde{k}_1(\zeta)$ are evaluated

$$\tilde{h}_1(\zeta) = \frac{2\zeta^3 - 5}{9\zeta^2}, \quad \tilde{k}_1(\zeta) = \frac{14\zeta^3 - 5}{9\zeta^2}. \quad (4.8)$$

We shall concentrate on the simplest non-abelian $N_f = 2$ case. With the final goal of comparing the theoretical results to the experimental data of baryons, it makes sense to choose this case, since the up and down quarks have almost the same mass and are much lighter than a strange quark. The $U(2)$ gauge field is decomposed,

$$\mathcal{A} = A + \frac{1}{\sqrt{2N_f}} \hat{A} = A + \frac{1}{2} \hat{A}, \quad (4.9)$$

where A and \hat{A} denote the $SU(2)$ and $U(1)$ gauge fields respectively. The Chern-Simon action (2.7) with the rescaling (4.3) is written down as

$$S_{\text{CS}} = \frac{27\pi\kappa}{8\lambda} \epsilon^{\alpha_1\alpha_2\alpha_3\alpha_4\alpha_5} \int d^4x d\tilde{z} \left[\hat{A}_{\alpha_1} \text{tr}(F_{\alpha_2\alpha_3} F_{\alpha_4\alpha_5}) + \frac{1}{6} \hat{A}_{\alpha_1} \hat{F}_{\alpha_2\alpha_3} \hat{F}_{\alpha_4\alpha_5} \right] \quad (4.10)$$

up to total derivatives. The indices α_i are 0, 1, 2, 3, \tilde{z} and $\epsilon^{0123\tilde{z}} = 1$.

The action of the gauge fields considered in this paper is constructed from (4.5) and (4.10),

$$S_{\text{gauge}} = S_{\text{YM}} + S_{\text{CS}}. \quad (4.11)$$

This action leads to the following equations of motion for the gauge fields:

$$\tilde{h}(\tilde{z})D_\nu F^{\mu\nu} + D_{\tilde{z}}(\tilde{k}(\tilde{z})F^{\mu\tilde{z}}) = \frac{27\pi\kappa}{8\lambda\tilde{\kappa}}\epsilon^{\mu\alpha_1\alpha_2\alpha_3\alpha_4}\hat{F}_{\alpha_1\alpha_2}F_{\alpha_3\alpha_4}, \quad (4.12a)$$

$$\tilde{k}(\tilde{z})D_\mu F^{\tilde{z}\mu} = \frac{27\pi\kappa}{8\lambda\tilde{\kappa}}\epsilon^{\tilde{z}\mu_1\mu_2\mu_3\mu_4}\hat{F}_{\mu_1\mu_2}F_{\mu_3\mu_4}, \quad (4.12b)$$

$$\tilde{h}(\tilde{z})\partial_\nu\hat{F}^{\mu\nu} + \partial_{\tilde{z}}(\tilde{k}(\tilde{z})\hat{F}^{\mu\tilde{z}}) = \frac{27\pi\kappa}{8\lambda\tilde{\kappa}}\epsilon^{\mu\alpha_1\alpha_2\alpha_3\alpha_4}\left[\text{tr}(F_{\alpha_1\alpha_2}F_{\alpha_3\alpha_4}) + \frac{1}{2}\hat{F}_{\alpha_1\alpha_2}\hat{F}_{\alpha_3\alpha_4}\right], \quad (4.12c)$$

$$\tilde{k}(\tilde{z})\partial_\mu\hat{F}^{\tilde{z}\mu} = \frac{27\pi\kappa}{8\lambda\tilde{\kappa}}\epsilon^{\tilde{z}\mu_1\mu_2\mu_3\mu_4}\left[\text{tr}(F_{\mu_1\mu_2}F_{\mu_3\mu_4}) + \frac{1}{2}\hat{F}_{\mu_1\mu_2}\hat{F}_{\mu_3\mu_4}\right], \quad (4.12d)$$

where μ_i, ν are 0, 1, 2, 3.

4.1. Baryon as instanton

Following [9], we now introduce the rescaling of the coordinates and the fields,

$$\begin{aligned} x^0 &= x_{(r)}^0, & x^i &= \frac{1}{\sqrt{\lambda}}x_{(r)}^i, & \tilde{z} &= \frac{1}{\sqrt{\lambda}}\tilde{z}_{(r)}, \\ \mathcal{A}_0 &= \mathcal{A}_{(r)0}, & \mathcal{A}_i &= \sqrt{\lambda}\mathcal{A}_{(r)i}, & \mathcal{A}_{\tilde{z}} &= \sqrt{\lambda}\mathcal{A}_{(r)\tilde{z}}, \end{aligned} \quad (4.13)$$

where $i = 1, 2, 3$, and consider the expansion with respect to large λ . Under this expansion, we can approximate $\tilde{h}(\tilde{z}_{(r)}/\sqrt{\lambda}; \zeta) \approx 1$ and $\tilde{k}(\tilde{z}_{(r)}/\sqrt{\lambda}; \zeta) \approx 1$ from (4.7). The equations of motion (4.12) are then reduced at the leading order of λ to

$$D_M^{(r)}F_{(r)}^{NM} = 0, \quad (4.14a)$$

$$D_M^{(r)}F_{(r)}^{0M} = \frac{27\pi\kappa}{8\tilde{\kappa}}\epsilon_{MNPQ}\hat{F}_{(r)}^{MN}F_{(r)}^{PQ}, \quad (4.14b)$$

$$\partial_M^{(r)}\hat{F}_{(r)}^{NM} = 0, \quad (4.14c)$$

$$\partial_M^{(r)}\hat{F}_{(r)}^{0M} = \frac{27\pi\kappa}{8\tilde{\kappa}}\epsilon_{MNPQ}\left[\text{tr}\left(F_{(r)}^{MN}F_{(r)}^{PQ}\right) + \frac{1}{2}\hat{F}_{(r)}^{MN}\hat{F}_{(r)}^{PQ}\right], \quad (4.14d)$$

where $M, N, P, Q = 1, 2, 3, \tilde{z}$. Since (4.14a) is a four-dimensional instanton equation, its classical solution can be described as BPST instanton [41],

$$\begin{aligned} A_M^{\text{cl}}(x^i, \tilde{z}) &= \left(= \sqrt{\lambda}\mathcal{A}_{(r)M}(x_{(r)}^i, \tilde{z}_{(r)}) \right) = -iv(\xi)g\partial_M g^{-1} \\ v(\xi) &= \frac{\xi^2}{\xi^2 + \rho^2}, & \xi &= \sqrt{(x^i - X^i)^2 + (\tilde{z} - \tilde{Z})^2}, \\ g(x^i, z) &= \frac{(\tilde{z} - \tilde{Z})\mathbf{1} - i(x^i - X^i)\tau_i}{\xi}. \quad (i = 1, 2, 3) \end{aligned} \quad (4.15)$$

The field strength of A_M^{cl} are calculated as

$$F_{ij}^{\text{cl}} = \frac{2\rho^2}{(\xi^2 + \rho^2)^2} \epsilon^{ija} \tau_a, \quad F_{\tilde{z}j}^{\text{cl}} = \frac{2\rho^2}{(\xi^2 + \rho^2)^2} \tau_j.$$

This solution is a one-instanton solution. In a similar way we can write a 't Hooft multi-instanton solution. The equations (4.14*b, c*) lead to

$$A_0^{\text{cl}} = \hat{A}_M^{\text{cl}} = 0 \tag{4.16}$$

with an appropriate gauge fixing. Substituting the solutions (4.15) and (4.16) into the equation of motion for \hat{A}_0 (4.14*d*), we obtain

$$\partial_M^2 \hat{A}_0 = -\frac{648\pi\kappa}{\lambda\tilde{\kappa}} \frac{\rho^4}{(\xi^2 + \rho^2)^4},$$

which can be solved,

$$\hat{A}_0^{\text{cl}} = \frac{27\pi\kappa}{\lambda\tilde{\kappa}} \frac{\xi^2 + 2\rho^2}{(\xi^2 + \rho^2)^2}. \tag{4.17}$$

Here we should note that the ζ dependence is included in the factor $\kappa/\tilde{\kappa} = \zeta^{-1}$. This factor does not appear in the other gauge fields A_0, A_M, \hat{A}_M and these fields are in the order of λ^0 . On the other hand, \hat{A}_0 is in the order of λ^{-1} , that is to say, the ζ dependence is derived from the λ^{-1} correction.

In terms of the classical solutions (4.15), (4.16) and (4.17), one can compute the mass of the baryon M , which depends on the moduli parameters ρ, Z via $S = -\int dt M$ from the action (4.11),

$$\begin{aligned} M &= 8\pi^2 \tilde{\kappa} \left[1 + \frac{\tilde{h}_1 + \tilde{k}_1}{2} \left(\tilde{Z}^2 + \frac{\rho^2}{2} \right) + \left(\frac{27\pi\kappa}{\lambda\tilde{\kappa}} \right)^2 \frac{1}{5\rho^2} \right] \\ &= 8\pi^2 \kappa \zeta \left(1 + \frac{1}{3\zeta^2} Z^2 + \frac{8\zeta^3 - 5}{18\zeta^2} \rho^2 + \frac{729\pi^2}{5\lambda^2 \zeta^2} \frac{1}{\rho^2} \right), \end{aligned}$$

where we used (4.8). Then we can find the critical values of the moduli parameters so that M is minimized,

$$Z_{\text{cr}} = 0, \quad \rho_{\text{cr}}^2 = \frac{81\pi}{\lambda} \sqrt{\frac{2}{40\zeta^3 - 25}}, \tag{4.18}$$

and the minimum value of M becomes

$$M_{\text{min}} = 8\pi^2 \kappa \left(\zeta + \frac{18\pi}{\lambda\zeta} \sqrt{\frac{8\zeta^3 - 5}{10}} \right).$$

From the expression of ρ_{cr} we thus see that generalizing the anit-podal case to the $\zeta \geq 1$ family of models does not improve the situation that the size of the baryon scales like $\sim 1/\sqrt{\lambda}$ and hence stringy corrections can play a role in the game.

The same kind of analysis can be done in the non-critical holographic model in six dimensions [42,38]. This will be discussed in Section 6.

4.2. Mass spectra

The study of the mass spectra of the baryons is also very similar to the one in [9]. The idea is to introduce the collective coordinates associated with the instanton solution and to semi-classically quantize them. The collective coordinates of instanton span a moduli space with a topology of $\mathbb{R}^4 \times (\mathbb{R}^4/\mathbb{Z}_2)$. The moduli are the position (X^i, Z) , the size $\rho = \sqrt{y_1^2 + \dots + y_4^2}$ and the $SU(2)$ orientation $a_I := y_I/\rho$ ($I = 1, \dots, 4$). As usual the basic assumption of the semi-classical quantization is that the collective coordinates $X^\alpha := (X^i, Z, y_I)$ depend on time.

Thus the fluctuations of $SU(2)$ gauge fields are described as

$$A_M(t, x) = V(t, x^i)A_M^{\text{cl}}(x^i, z; X^\alpha(t))V^{-1}(t, x^i) - iV(t, x^i)\partial_M V^{-1}(t, x^i),$$

where A_M^{cl} has been given by (4.15). The equation of motion (4.14b) determines $\Phi := -iV^{-1}\dot{V}$ as

$$\begin{aligned} \Phi(t, x) &= -\dot{X}^i(t)A_i^{\text{cl}}(x) - \dot{Z}(t)A_z^{\text{cl}}(x) + \chi^a(t)\Phi_a(x), \\ \chi^a &= 2(a_4\dot{a}_a - \dot{a}_4a_a + \epsilon^{abc}a_b\dot{a}_c), \quad \Phi_a = \frac{1}{2}v(\xi)g\tau_a g^{-1}. \end{aligned} \quad (4.19)$$

In terms of these equations, the field strength of the $SU(2)$ gauge field is written as $F_{MN} = VF_{MN}^{\text{cl}}V^{-1}$ and $F_{0M} = V(\dot{X}^N F_{MN}^{\text{cl}} + \dot{\rho}\partial_\rho A_M^{\text{cl}} - \chi^a D_M^{\text{cl}}\Phi_a)V^{-1}$. The equation of motion (4.14d) with this solution of A_M does not change \hat{A}_0 , that is, $\hat{A}_0 = \hat{A}_0^{\text{cl}}$.

Substituting the gauge fields obtained so far into the action (4.5), derives a Lagrangian of the collective coordinates which is the same as in [9],

$$L = -m_0 + \frac{1}{2}m_X\dot{\vec{X}}^2 + \frac{1}{2}m_Z\dot{Z}^2 - \frac{1}{2}m_Z\omega_Z^2 Z^2 + \frac{1}{2}m_y\dot{\vec{y}}^2 - \frac{1}{2}m_y\omega_\rho^2\rho^2 - \frac{Q}{\rho^2}, \quad (4.20)$$

where $\dot{\vec{y}}^2 = \dot{\rho}^2 + \rho^2\dot{\vec{a}}^2$ apart from the fact that the various mass parameters are now ζ dependent as follows

$$m_0 = m_X = 8\pi^2\tilde{\kappa} = 8\pi^2\kappa\zeta, \quad (4.21a)$$

$$m_Z = 8\pi^2\kappa\frac{3\zeta}{8\zeta^3 - 5}, \quad \omega_Z^2 = \frac{16\zeta^3 - 10}{9\zeta^2}, \quad (4.21b)$$

$$m_y = 16\pi^2\kappa\zeta, \quad \omega_\rho^2 = \frac{8\zeta^3 - 5}{18\zeta^2}, \quad Q = 8\pi^2\kappa\frac{729\pi^2}{5\lambda^2\zeta}. \quad (4.21c)$$

The system is then quantized in the same way as [9]. Using the canonical momenta, the corresponding Hamiltonian becomes $H = -(2m_0)^{-1}(\partial/\partial\vec{X})^2 - (2m_0)^{-1}(\partial/\partial\vec{Z})^2 - (4m_0)^{-1}(\partial/\partial\vec{y})^2 + U$. The isospin and spin currents are defined by

$$I_a = \frac{i}{2} \left(y_4 \frac{\partial}{\partial y_a} - y_a \frac{\partial}{\partial y_4} - \epsilon_{abc} y_b \frac{\partial}{\partial y_c} \right), \quad (4.22)$$

$$J_a = \frac{i}{2} \left(-y_4 \frac{\partial}{\partial y_a} + y_a \frac{\partial}{\partial y_4} - \epsilon_{abc} y_b \frac{\partial}{\partial y_c} \right). \quad (4.23)$$

For a baryon which is located at $\vec{X} = 0$, in other words, the baryon is static with respect to fluctuations in the ordinary four-dimensional spacetime. The energy spectra of the fluctuations of Z and \vec{y} take the following form

$$E_y = \omega_\rho \left(\sqrt{(l+1)^2 + 2m_y Q} + 2n_\rho + 1 \right), \quad E_Z = \omega_Z \left(n_z + \frac{1}{2} \right), \quad (4.24)$$

and hence, using (4.21), the baryon mass formula is given by

$$\begin{aligned} M_{l,n_\rho,n_z} &= m_0 + E_y + E_Z \\ &= 8\pi^2 \kappa \zeta + \sqrt{\frac{8\zeta^3 - 5}{3\zeta^2}} \left[\sqrt{\frac{(l+1)^2}{6} + \frac{2N_c^2}{15}} + \frac{2(n_\rho + n_z) + 2}{\sqrt{6}} \right]. \end{aligned} \quad (4.25)$$

l is a positive odd integer and describes a spin J and an isospin I as $I = J = l/2$. For later convenience, we write down the wave functions of proton $|p \uparrow\rangle$ and neutron $|n \uparrow\rangle$,

$$|p \uparrow\rangle \propto R(\rho; \zeta) \psi_Z(Z; \zeta) (a_1 + ia_2), \quad |n \uparrow\rangle \propto R(\rho; \zeta) \psi_Z(Z; \zeta) (a_4 + ia_3), \quad (4.26)$$

$$R(\rho; \zeta) = \rho^{-1+2\sqrt{1+N_c^2/5}} \exp\left(-m_0 \sqrt{\frac{8\zeta^3 - 5}{18\zeta^2}} \rho^2\right), \quad (4.27a)$$

$$\psi_Z(Z; \zeta) = \exp\left(-\frac{m_0}{\sqrt{2\zeta^2(8\zeta^3 - 5)}} Z^2\right). \quad (4.27b)$$

At this point we would like to compare the baryon masses and in particular the mass differences between the various baryonic states. For this purpose we first have to turn on back M_{KK} . If we identify the modes of $(l, n_\rho, n_z) = (1, 0, 0)$ and $(3, 0, 0)$ with $n(940)$ and $\Delta(1232)$ (see also Table 1), ζ and M_{KK} satisfy

$$\frac{N_c \lambda}{27\pi} \zeta + \sqrt{\frac{8\zeta^3 - 5}{3\zeta^2}} \left(\sqrt{\frac{2}{3} + \frac{6}{5}} + \sqrt{\frac{2}{3}} \right) = \frac{940}{M_{\text{KK}}}, \quad (4.28)$$

$$\frac{N_c \lambda}{27\pi} \zeta + \sqrt{\frac{8\zeta^3 - 5}{3\zeta^2}} \left(\sqrt{\frac{8}{3} + \frac{6}{5}} + \sqrt{\frac{2}{3}} \right) = \frac{1232}{M_{\text{KK}}}. \quad (4.29)$$

We can read from these equations,

$$M_{\text{KK}} \sqrt{\frac{8\zeta^3 - 5}{3\zeta^2}} = \frac{292\sqrt{15}}{\sqrt{58} - \sqrt{28}}. \quad (4.30)$$

Since the left hand side of this equation is the monotonically increasing function of ζ , the Kaluza-Klein mass M_{KK} is bounded as

$$M_{\text{KK}} \leq \frac{292\sqrt{15}}{\sqrt{58} - \sqrt{28}} \approx 487 \text{ [MeV]}. \quad (4.31)$$

In terms of (4.28) (or (4.29)) and (4.30), we can now compute the baryon masses $M_{\text{KK}}M_{l,n_\rho,n_z}$ [MeV], which are shown in Table 2 and compare them to the experimental data of Table 1. This is done by first fixing $N_c = 3$.

| N baryons | $I(J^P)$ | Δ baryons | $I(J^P)$ |
|-------------|------------------------------|------------------|------------------------------|
| $n(940)$ | $\frac{1}{2}(\frac{1}{2}^+)$ | $\Delta(1232)$ | $\frac{3}{2}(\frac{3}{2}^+)$ |
| $N(1440)$ | $\frac{1}{2}(\frac{1}{2}^+)$ | $\Delta(1600)$ | $\frac{3}{2}(\frac{3}{2}^+)$ |
| $N(1535)$ | $\frac{1}{2}(\frac{1}{2}^-)$ | $\Delta(1700)$ | $\frac{3}{2}(\frac{3}{2}^-)$ |
| $N(1650)$ | $\frac{1}{2}(\frac{1}{2}^-)$ | $\Delta(1920)$ | $\frac{3}{2}(\frac{3}{2}^+)$ |
| $N(1710)$ | $\frac{1}{2}(\frac{1}{2}^+)$ | $\Delta(1940)$ | $\frac{3}{2}(\frac{3}{2}^-)$ |
| $N(2090)$ | $\frac{1}{2}(\frac{1}{2}^-)$ | | |
| $N(2100)$ | $\frac{1}{2}(\frac{1}{2}^+)$ | | |

Table 1: The experimental data of baryon mass spectra [43].

| N baryons | (n_ρ, n_z) | $M_{\text{KK}}M_{1,n_\rho,n_z}$ | Δ baryons | (n_ρ, n_z) | $M_{\text{KK}}M_{3,n_\rho,n_z}$ |
|-------------|-----------------|---------------------------------|------------------|-----------------|---------------------------------|
| $n(940)$ | (0, 0) | 940 | $\Delta(1232)$ | (0, 0) | 1232 |
| $N(1440)$ | (1, 0) | 1337 | $\Delta(1600)$ | (1, 0) | 1629 |
| $N(1535)$ | (0, 1) | 1337 | $\Delta(1700)$ | (0, 1) | 1629 |
| $N(1650)$ | (1, 1) | 1735 | $\Delta(1920)$ | (2, 0), (0, 2) | 2027 |
| $N(1710)$ | (2, 0), (0, 2) | 1735 | $\Delta(1940)$ | (1, 1) | 2027 |
| $N(2090)$ | (2, 1), (0, 3) | 2132 | | | |
| $N(2100)$ | (1, 2), (3, 0) | 2132 | | | |

Table 2: The baryon mass spectra in our model.

Since the $1/N_c$ corrections are important for the states of larger quantum numbers, it is physically better to fit the baryon mass formula (4.25) to the experimental data by using

the lower quantum numbers. But here instead we determine the masses by using a best fit approach, namely, minimizing χ^2 with respect to the all states listed in Table 1. We need to determine the two parameters A and B which are defined from (4.25) by

$$M_{\text{KK}}M_{l,n_\rho,n_z} = A + B \left[\sqrt{\frac{(l+1)^2}{6} + \frac{6}{5}} + \frac{2(n_\rho + n_z) + 2}{\sqrt{6}} \right],$$

$$A := \frac{M_{\text{KK}}\lambda}{9\pi}\zeta, \quad B := M_{\text{KK}}\sqrt{\frac{8\zeta^3 - 5}{3\zeta^2}}.$$

Though we should take care of the zero point energy, here it can be absorbed into A . Then $(A, B) = (99.9, 424.8)$ is the best fit. This implies that λ is not large and hence $1/\lambda$ corrections may not be negligible. The Kaluza-Klein mass is bounded so that $M_{\text{KK}} \leq 424.8$ [MeV]. The mass spectra evaluated in terms of these values are shown in Table 3.

| N baryons | (n_ρ, n_z) | $M_{\text{KK}}M_{1,n_\rho,n_z}$ | Δ baryons | (n_ρ, n_z) | $M_{\text{KK}}M_{3,n_\rho,n_z}$ |
|-------------|-----------------|---------------------------------|------------------|-----------------|---------------------------------|
| $n(940)$ | (0, 0) | 1027 | $\Delta(1232)$ | (0, 0) | 1282 |
| $N(1440)$ | (1, 0) | 1374 | $\Delta(1600)$ | (1, 0) | 1629 |
| $N(1535)$ | (0, 1) | 1374 | $\Delta(1700)$ | (0, 1) | 1629 |
| $N(1650)$ | (1, 1) | 1721 | $\Delta(1920)$ | (2, 0), (0, 2) | 1976 |
| $N(1710)$ | (2, 0), (0, 2) | 1721 | $\Delta(1940)$ | (1, 1) | 1976 |
| $N(2090)$ | (2, 1), (0, 3) | 2068 | | | |
| $N(2100)$ | (1, 2), (3, 0) | 2068 | | | |

Table 3: The baryon masses by the use of the minimal χ^2 fitting.

Since there are more degeneracies for the states with larger quantum numbers, the χ^2 -fitted data are strongly affected by these states.

4.3. Mean radii, magnetic moments and couplings

Next we should like to determine the impact of $\zeta \neq 1$ on the baryonic properties of the mean radii, magnetic moments and various couplings. For that purpose we consider the currents of the $U(N_f)_L \times U(N_f)_R$ chiral symmetry in the same way as was done in [37]. On account of the gauge configuration

$$\mathcal{A}_\alpha(x^\mu, \tilde{z}) = \mathcal{A}_\alpha^{\text{cl}}(x^\mu, \tilde{z}) + \delta\mathcal{A}_\alpha(x^\mu, \tilde{z}),$$

$$\delta\mathcal{A}_\alpha(x^\mu, +\infty) = \mathcal{A}_{L\mu}(x^\mu), \quad \delta\mathcal{A}_\alpha(x^\mu, -\infty) = \mathcal{A}_{R\mu}(x^\mu),$$

we can read the currents from the action (4.11),

$$S_{\text{gauge}} = -2 \int d^4x \text{Tr}(A_{L\mu} \mathcal{J}_L^\mu + A_{R\mu} \mathcal{J}_R^\mu) + \mathcal{O}(\delta\mathcal{A}^2),$$

where

$$\mathcal{J}_{L\mu} = -\tilde{\kappa} \left(\tilde{k}(\tilde{z}) \mathcal{F}_{\mu\tilde{z}}^{\text{cl}} \right) \Big|_{\tilde{z}=+\infty}, \quad \mathcal{J}_{R\mu} = \tilde{\kappa} \left(\tilde{k}(\tilde{z}) \mathcal{F}_{\mu\tilde{z}}^{\text{cl}} \right) \Big|_{\tilde{z}=-\infty}. \quad (4.32)$$

Obviously from the left and right currents one can form the vector and axial currents as follows,

$$\mathcal{J}_{V\mu} = \mathcal{L}_{L\mu} + \mathcal{J}_{R\mu} = -\tilde{\kappa} \left[\tilde{k}(\tilde{z}) \mathcal{F}_{\mu\tilde{z}}^{\text{cl}} \right]_{\tilde{z}=-\infty}^{\tilde{z}=+\infty}, \quad (4.33)$$

$$\mathcal{J}_{A\mu} = \mathcal{L}_{L\mu} - \mathcal{J}_{R\mu} = -\tilde{\kappa} \left[\tilde{k}(\tilde{z}) \mathcal{F}_{\mu\tilde{z}}^{\text{cl}} \psi_0(\tilde{z}) \right]_{\tilde{z}=-\infty}^{\tilde{z}=+\infty}. \quad (4.34)$$

$\psi_0(\tilde{z})$ is defined by $\psi_0(\tilde{z}) := \xi(\tilde{z})/\xi(\infty)$ in terms of the function $\xi(\tilde{z})$ satisfying the equation $\tilde{k}(\tilde{z})\partial_{\tilde{z}}\xi(\tilde{z}) = 1$. $\xi(\tilde{z})$ can be rewritten as

$$\xi(\tilde{z}) = \int_0^{\tilde{z}} \frac{d\tilde{z}'}{\tilde{k}(\tilde{z}')}, \quad (4.35)$$

because $\xi(\tilde{z})$ is an odd function and $\xi(0) = 0$. Then $\psi_0(\tilde{z})$ has the property of $\psi_0(\pm\infty) = \pm 1$. The currents are also decomposed as the gauge fields (4.9) to the $SU(2)$ and $U(1)$ parts, $\mathcal{J}^\mu = J^\mu + (1/2)\hat{J}^\mu$. In order to evaluate the currents (4.33) and (4.34), it is necessary to understand the behavior of the gauge field strengths at the UV boundary, $\tilde{z} = \pm\infty$. But so far we know the expression of the gauge field strengths only in the region of $\tilde{z} \ll 1$. Ref.[37] has succeeded in extending it to the large \tilde{z} region in the anti-podal case ($\zeta = 1$). In the same way, we can easily evaluate in the non-anti-podal case the gauge field strengths for $\tilde{Z} \ll 1 \ll \tilde{z}$,

$$F_{0\tilde{z}} \approx 2\pi^2 \partial_0 (\rho^2 \mathbf{a} \tau^a \mathbf{a}^{-1}) \partial_a H - 4\pi^2 i \rho^2 \mathbf{a} \mathbf{a}^{-1} \partial_{\tilde{z}} G \\ - 2\pi^2 \rho^2 \mathbf{a} \tau^a \mathbf{a}^{-1} \dot{X}^i \{ (\partial_i \partial_a - \delta_{ia} \partial_j^2) H - \epsilon_{iaj} \partial^j \partial_{\tilde{z}} G \}, \quad (4.36a)$$

$$F_{i\tilde{z}} \approx 2\pi^2 \rho^2 \mathbf{a} \tau^a \mathbf{a}^{-1} \{ (\partial_i \partial_a - \delta_{ia} \partial_j^2) H - \epsilon_{iaj} \partial^j \partial_{\tilde{z}} G \}, \quad (4.36b)$$

$$\hat{F}_{0\tilde{z}} \approx \frac{108\pi^3 \kappa}{\lambda \tilde{\kappa}} \partial_{\tilde{z}} G, \quad (4.36c)$$

$$\hat{F}_{i\tilde{z}} \approx \frac{108\pi^3 \kappa}{\lambda \tilde{\kappa}} \left[\dot{Z} \partial_i H - \dot{X}_i \partial_{\tilde{z}} G - \frac{\rho^2 \chi^a}{4} \{ (\partial_i \partial_a - \delta_{ia} \partial_j^2) H - \epsilon_{iaj} \partial^j \partial_{\tilde{z}} G \} \right], \quad (4.36d)$$

where $\mathbf{a} = a_4 + ia_a \tau^a$. H and G are the Green's functions generalised for the curved background,

$$G = \tilde{\kappa} \sum_{n=1}^{\infty} \psi_n(\tilde{z}) \psi_n(\tilde{Z}) Y_n(|\vec{x} - \vec{X}|), \quad H = \tilde{\kappa} \sum_{n=0}^{\infty} \phi_n(\tilde{z}) \phi_n(\tilde{Z}) Y_n(|\vec{x} - \vec{X}|). \quad (4.37)$$

The eigen functions ψ_n 's are defined by

$$-\tilde{h}(\tilde{z})^{-1} \partial_{\tilde{z}} (\tilde{k}(\tilde{z}) \partial_{\tilde{z}} \psi_n) = \lambda_n \psi_n, \quad \tilde{\kappa} \int d\tilde{z} \tilde{h}(\tilde{z}) \psi_m \psi_n = \delta_{mn}, \quad (4.38)$$

while ϕ_n 's are defined on account of (4.35) by

$$\phi_0(\tilde{z}) = \frac{1}{\sqrt{2\tilde{\kappa}\xi(\infty)\tilde{k}(\tilde{z})}}, \quad \phi_n(\tilde{z}) = \frac{1}{\sqrt{\lambda_n}} \partial_{\tilde{z}} \psi_n(\tilde{z}), \quad (n \in \mathbb{N}) \quad (4.39)$$

so that these modes satisfy the normalisation $\tilde{\kappa} \int d\tilde{z} \tilde{k}(\tilde{z}) \phi_m \phi_n = \delta_{mn}$ for $n, m \in \{0, \mathbb{N}\}$. Y_n denotes the Yukawa potential⁵

$$Y_n(r) = -\frac{1}{4\pi} \frac{e^{-\sqrt{\lambda_n} r}}{r}. \quad (4.40)$$

Mean square radii

The baryon number current is denoted in terms of the vector current (4.33) by

$$J_B^\mu = \frac{2}{N_c} \hat{J}_V^\mu = -\frac{2}{N_c} \tilde{\kappa} \left[\tilde{k}(\tilde{z}) \hat{F}^{\mu\tilde{z}} \right]_{\tilde{z}=-\infty}^{\tilde{z}=\infty}. \quad (4.41)$$

Since the baryon number N_B is calculated as $N_B = \int d^3x \langle J_B^0 \rangle = 1$, the baryon number density ρ_B with respect to the radial direction $r = |\vec{x} - \vec{X}|$ is described as

$$\rho_B(r) = 4\pi r^2 \langle J_B^0 \rangle = -4\pi r^2 \sum_{n=1}^{\infty} \left(\lambda_{2n-1} \tilde{\kappa} \int d\tilde{z} \tilde{h}(\tilde{z}) \psi_{2n-1}(\tilde{z}) \right) \psi_{2n-1}(\tilde{Z}) Y_{2n-1}(r). \quad (4.42)$$

Then the isoscalar mean square radius becomes

$$\begin{aligned} \langle r^2 \rangle_{I=0} &= \int_0^\infty dr r^2 \rho_B(r) \\ &= 6\tilde{\kappa} \sum_{n=1}^{\infty} \frac{1}{\lambda_{2n-1}} \int d\tilde{z} \tilde{h}(\tilde{z}) \psi_{2n-1}(\tilde{z}) \langle \psi_{2n-1}(\tilde{Z}) \rangle. \end{aligned} \quad (4.43)$$

⁵ The eigen equation in (4.38) is rewritten through (4.3) and (4.6) as $-h(z)^{-1} \partial_z (k(z) \partial_z \psi_n) = \lambda_n \psi_n$, which is exactly the eigen equation providing the meson mass spectra. That is to say, the meson mass m_n is denoted by $m_n = \sqrt{\lambda_n}$.

Since the baryon is almost localized at $\tilde{Z} = \tilde{Z}_{\text{cr}} = 0$ on account of (4.18) and (4.27b), $\langle \psi_{2n-1}(\tilde{Z}) \rangle$ can be approximated by $\psi_{2n-1}(0)$. Then, in the same way of [37], the isoscalar mean square radius is evaluated

$$\langle r^2 \rangle_{I=0} \approx \frac{1}{M_{\text{KK}}^2} \int_0^\infty d\tilde{z}' \frac{1}{\tilde{k}(\tilde{z}'; \zeta)} \int_0^{\tilde{z}'} d\tilde{z}'' 6\tilde{h}(\tilde{z}''; \zeta), \quad (4.44)$$

where we recovered the factor M_{KK} explicitly. One can numerically compute these integration and depict the results depending on ζ in fig. 5.

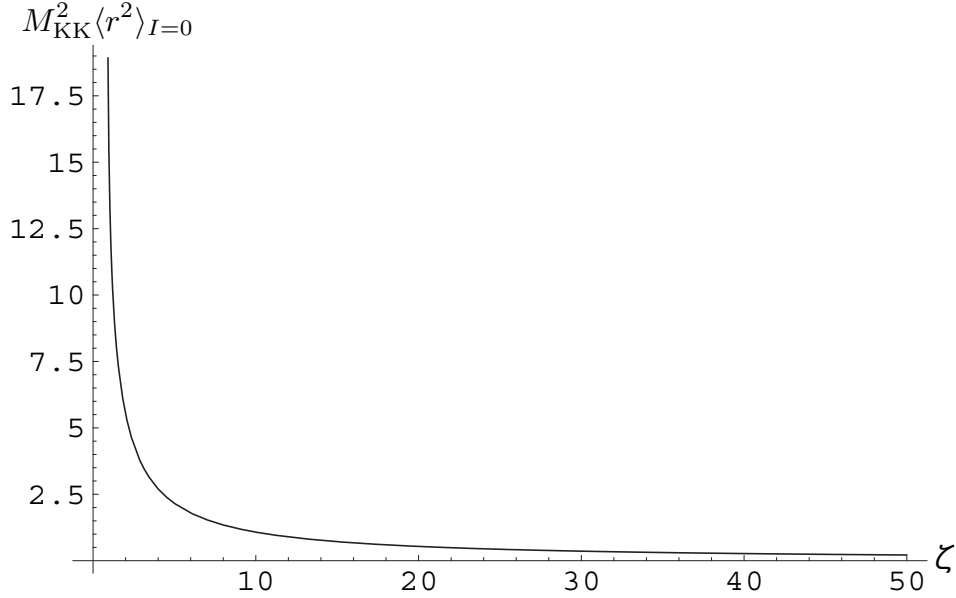


fig. 5 The ζ dependence of the isoscalar mean radius $M_{\text{KK}}^2 \langle r^2 \rangle_{I=0}$

The mean square radius (4.44) in the anti-podal case ($\zeta = 1$) has been calculated in [37], that is, $M_{\text{KK}}^2 \langle r^2 \rangle_{I=0} \approx 14.3$. If the mass scale M_{KK} is fixed, then the mean radius decreases with respect to ζ as can be seen in fig. 5.

From the isovector charge $Q_V = (\tau_a/2)Q_V^a$, we obtain from (4.33) and (4.36a)

$$\begin{aligned} Q_V^a &= \text{tr} \left(\tau^a \int d^3x J_V^0 \right) \\ &= - \int dr 4\pi r^2 I^a \sum_{n=1}^{\infty} \left(\lambda_{2n-1} \tilde{\kappa} \int d\tilde{z} \tilde{h}(\tilde{z}) \psi_{2n-1}(\tilde{z}) \right) \psi_{2n-1}(\tilde{Z}) Y_{2n-1}(r), \end{aligned} \quad (4.45)$$

where we used $4\pi^2 \tilde{\kappa} \rho^2 i \text{tr}(\tau^a \mathbf{a} \dot{\mathbf{a}}^{-1}) = I^a$, which is derived from (4.22). The isovector charge density $\rho_V(r)$ is defined by $Q_V^a = \int dr I^a \rho_V(r)$. Comparing (4.45) with (4.42), we can show that $\rho_V(r)$ is equal to the baryon number density $\rho_B(r)$. So the isovector mean square

charge radius is the same as the isoscalar mean square radius. This statement does not change from the $\zeta = 1$ case investigated by [37]. The electric mean square charge radii also have been mentioned in [37], where the mean radius for a proton $\langle r^2 \rangle_{E,p}$ and the one for a neutron $\langle r^2 \rangle_{E,n}$ become

$$\langle r^2 \rangle_{E,p} = \langle r^2 \rangle_{I=0}, \quad \langle r^2 \rangle_{E,n} = 0.$$

These equations are satisfied also in the non-anti-podal case.

Since the axial current (4.34) leads to

$$\int d^3x J_A \propto - \int dr 4\pi r^2 \sum_{n=1}^{\infty} \left(\lambda_{2n} \tilde{\kappa} \int d\tilde{z} \tilde{h}(\tilde{z}) \psi_{2n}(\tilde{z}) \psi_0(\tilde{z}) \right) \partial_{\tilde{Z}} \psi_{2n}(\tilde{Z}) Y_{2n}(r) = \frac{1}{\tilde{k}(\tilde{Z}) \xi(\infty)},$$

and also $\int d^3x J_A \propto \int dr \rho_A(r)$, the axial charge density $\rho_A(r)$ is defined by

$$\rho_A(r) = \frac{\left\langle 4\pi r^2 \sum_{n=1}^{\infty} \left(\lambda_{2n} \tilde{\kappa} \int d\tilde{z} \tilde{h}(\tilde{z}) \psi_{2n}(\tilde{z}) \psi_0(\tilde{z}) \right) \partial_{\tilde{Z}} \psi_{2n}(\tilde{Z}) Y_{2n}(r) \right\rangle}{\left\langle \frac{1}{\tilde{k}(\tilde{Z}) \xi(\infty)} \right\rangle}.$$

Now we shall approximate $\langle 1/\tilde{k}(\tilde{Z}) \rangle$ by the classical value $1/\tilde{k}(\tilde{Z}_{\text{cr}} = 0) = 1$. Then, in the way similar to [37], the axial radius $\langle r^2 \rangle_A = \int dr r^2 \rho_A(r)$ is described as

$$\langle r^2 \rangle_A = \frac{3}{M_{\text{KK}}^2} \int_{-\infty}^{\infty} d\tilde{z} \frac{1}{\tilde{k}(\tilde{z})} \int_0^{\tilde{z}} d\tilde{z}' \tilde{h}(\tilde{z}') \psi_0(\tilde{z}'). \quad (4.46)$$

In terms of (4.6) and (4.35) we can numerically evaluate $\langle r^2 \rangle_A$, and its behavior is depicted in fig. 6.⁶

⁶ The integrations in (4.46) are numerically done by Mathematica in terms of Monte-Carlo method.

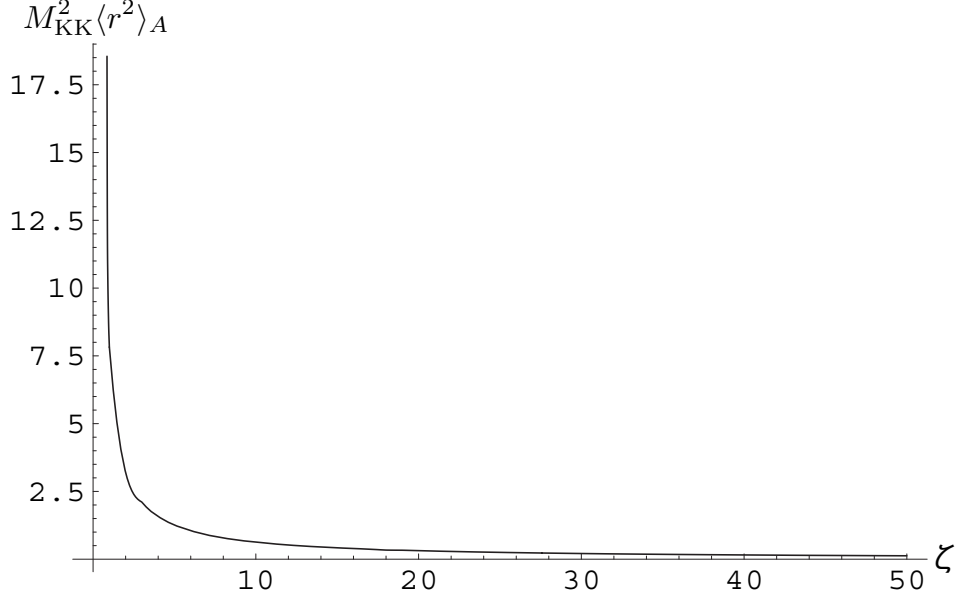


fig. 6 The ζ dependence of the axial charge mean radius $M_{\text{KK}}^2 \langle r^2 \rangle_A$.

From fig. 6, the axial charge mean radius is a monotonically decreasing function along ζ . Ref.[37] has calculated $M_{\text{KK}}^2 \langle r^2 \rangle_A \approx 7.82$ in $\zeta = 1$.

Magnetic moments

In terms of the baryon number current (4.41), the isoscalar magnetic moment is denoted by

$$\mu_{I=0}^i = \frac{1}{2} \epsilon^i{}_{jk} \int d^3x x^j J_B^k = -\frac{\rho^2 \chi^i}{4}, \quad (4.47)$$

where χ^i can be described from (4.19) and (4.23) as

$$\chi^i = \frac{1}{8\pi^2 \tilde{\kappa}} J^i.$$

Here we concentrate on the up-spin proton and neutron states, which have the spin $(J^1, J^2, J^3) = (0, 0, 1/2)$ and the mass $M_N^{\text{exp}} \approx 940$ [MeV]. By defining the g factor as $\mu_{I=0}^i = g_{I=0}(\tau^i/4M_N)$, we can identify the g factor as

$$g_{I=0} = \frac{M_N}{8\pi^2 \tilde{\kappa} M_{\text{KK}}}. \quad (4.48)$$

We should note that the ζ -dependence is included in $\tilde{\kappa}$, which is determined through the pion decay constant $f_\pi^{\text{exp}} \approx 92.4$ [MeV],

$$\left(\frac{f_\pi^{\text{exp}}}{M_{\text{KK}}} \right)^2 = \frac{4\tilde{\kappa}}{\pi^2} \int d\tilde{z} \frac{1}{\tilde{k}(\tilde{z}; \zeta)}. \quad (4.49)$$

This equation is read from the mode expansion of (4.2) for the pion field [7]. The isoscalar magnetic moment $g_{I=0}$ can be rewritten as

$$g_{I=0} = \frac{M_{\text{KK}}M_N}{2\pi^4 f_\pi^2} \int_{-\infty}^{\infty} d\tilde{z} \frac{1}{\tilde{k}(\tilde{z}; \zeta)}. \quad (4.50)$$

The ζ -dependence of $g_{I=0}$ is proportional to $\int d\tilde{z} \tilde{k}(\tilde{z}; \zeta)^{-1}$, which is depicted in fig. 7.

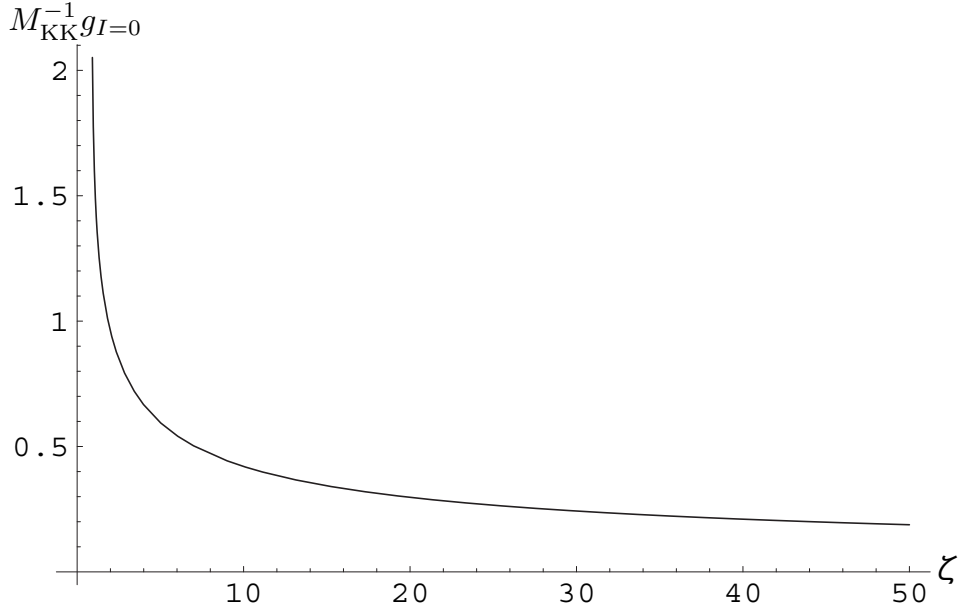


fig. 7 The plot of $M_{\text{KK}}^{-1}g_{I=0}(\zeta)$.

The isovector magnetic moment is given by

$$\mu_{I=1}^i = \epsilon^i_{jk} \int d^3x x^j \text{tr}(J_V^k \tau^3) = -4\pi^2 \tilde{\kappa} \rho^2 \text{tr}(\mathbf{a} \tau^i \mathbf{a}^{-1} \tau^3), \quad (4.51)$$

We can evaluate (4.51) for the up-spin proton and neutron states as

$$\langle \mu_{I=1}^i \rangle_p = -\langle \mu_{I=1}^i \rangle_n = \frac{8\pi^2 \tilde{\kappa}}{3} \langle \rho^2 \rangle \delta^{3i}.$$

$\langle \rho^2 \rangle$ is calculated in terms of the wave function (4.27a)

$$\langle \rho^2 \rangle = \frac{\int d\rho \rho^5 R(\rho)^2}{\int d\rho \rho^3 R(\rho)^2} = \frac{\sqrt{5} + 2\sqrt{5 + N_c^2}}{2N_c} \rho_{\text{cr}}^2(\zeta),$$

where ρ_{cr} has been calculated in (4.18). Since the $g_{I=1}$ factor is defined in the same way as the isovector magnetic moment, we obtain

$$g_{I=1} = \frac{2\sqrt{2}M_N}{M_{\text{KK}}} \left(1 + 2\sqrt{1 + \frac{N_c^2}{5}} \right) \frac{\zeta}{\sqrt{8\zeta^3 - 5}}. \quad (4.52)$$

The function $M_{\text{KK}g_{I=1}}$ of ζ with $N_c = 3$ is drawn in the following figure:

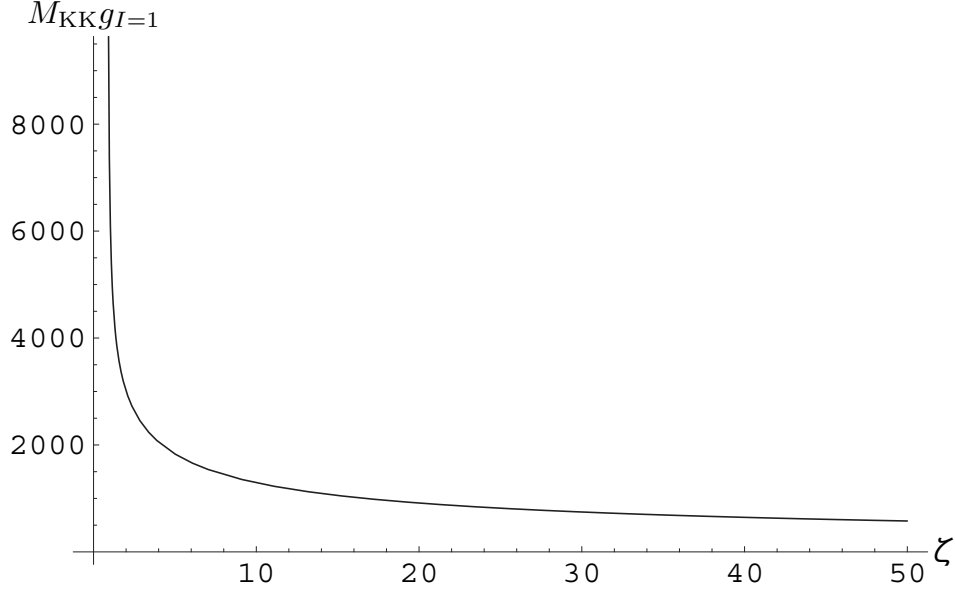


fig. 8 The plot of $M_{\text{KK}g_{I=1}}(\zeta)$ with $M_N = 940$ and $N_c = 3$.

By the use of (4.50) and (4.52), the magnetic moments for a proton and a neutron can be easily computed as $\mu_p = (g_{I=0} + g_{I=1})/4$ and $\mu_n = (g_{I=0} - g_{I=1})/4$ respectively.

Couplings

The axial coupling g_A is defined in terms of the axial current J_A^i in (4.34) as

$$\int d^3x \langle J_A^{a,i} \rangle = \frac{1}{2} g_A \langle \text{tr}(\mathbf{a} \tau^i \mathbf{a}^{-1} \tau^a) \rangle, \quad (4.53)$$

where $J_A^{a,i} = \text{tr}(\tau^a J_A^i)$. Since the left hand side of (4.53) is calculated from (4.32), (4.34) and (4.36b),

$$\int d^3x \langle J_A^{a,i} \rangle = \frac{8\pi^2 \tilde{\kappa}}{6\xi(\infty)} \left\langle \frac{\rho^2}{\tilde{k}(\tilde{Z})} \right\rangle \langle \text{tr}(\mathbf{a} \tau^i \mathbf{a}^{-1} \tau^a) \rangle,$$

one can read the axial coupling

$$g_A(\zeta) = \frac{8\pi^2 \tilde{\kappa}}{3\xi(\infty)} \left\langle \frac{\rho^2}{\tilde{k}(\tilde{Z})} \right\rangle \approx \frac{\sqrt{2} N_c}{\xi(\infty)} \frac{\zeta}{\sqrt{40\zeta^3 - 25}}. \quad (4.54)$$

The approximation was given by the classical values, that is, $\rho \approx \rho_{\text{cr}}$ and $\tilde{k}(\tilde{Z}) \approx \tilde{k}(\tilde{Z}_{\text{cr}}) = 1$ with (4.18). We should note that $\xi(\infty)$ also depends on ζ and can be numerically computed from (4.35). Then $g_A(\zeta)$ with $N_c = 3$ can be drawn as fig. 9.

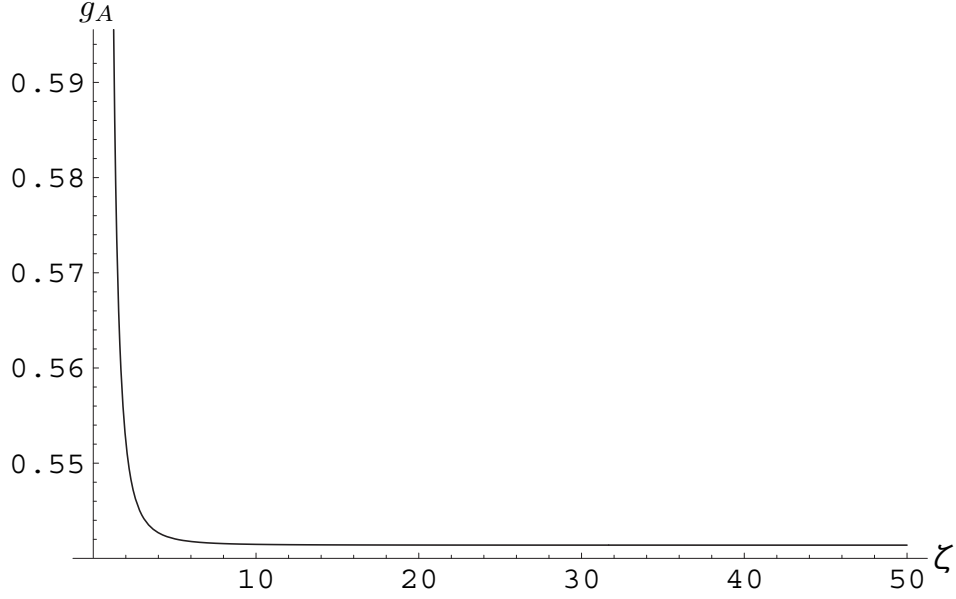


fig. 9 The plot of $g_A(\zeta)$ with $N_c = 3$.

In the anti-podal case, [37] evaluated the axial coupling, $g_A(\zeta = 1) \approx 0.697$. Since (4.54) is independent of M_{KK} , we shall compare $g_A(\zeta)$ with the experimental datum g_A^{exp} , which is approximately equal to 1.27. If we set $g_A(\zeta) \approx 1.27$, then (4.54) leads to $\zeta \approx 0.870$. But this solution is nonsense, because ζ must be in $[1, \infty)$ by definition. At present, the best fitted value of ζ for the experimental data is $\zeta = 1$, that is, the anti-podal SS model. We shall give more comments on this issue in Section 7.

4.4. M_{KK} and ζ fitted to experimental data

So far we have calculated the baryon mass spectra, the mean radii, the magnetic moments and the couplings as functions of M_{KK} and ζ . Comparing those quantities with the experimental data, we shall determine M_{KK} and ζ . We remind the reader that for $\zeta = 1$ these properties of the baryons were computed in [37]. The idea is to find the values of M_{KK} and ζ that yield the best fit to the experimental data. We shall extract the relation between M_{KK} and ζ in five different ways from the baryonic data and in two more ways from the mesonic spectra.

We start with the mass difference (4.30) between the nucleon, $n(940)$, and the lowest mode of Δ -baryon, $\Delta(1232)$, from which we find the following relation between M_{KK} and ζ :

$$M_{\text{KK}} = \frac{876\sqrt{5}}{\sqrt{58} - \sqrt{28}} \frac{\zeta}{\sqrt{8\zeta^3 - 5}} =: \mathcal{B}_1(\zeta). \quad (4.55)$$

Next we use the isoscalar mean square radius (4.44) to obtain

$$M_{\text{KK}} = \sqrt{\frac{6}{\langle r^2 \rangle_{I=0}^{\text{exp}}} \int_0^\infty d\tilde{z}' \tilde{k}(\tilde{z}'; \zeta)^{-1} \int_0^{\tilde{z}'} d\tilde{z}'' \tilde{h}(\tilde{z}''; \zeta)} =: \mathcal{B}_2(\zeta), \quad (4.56)$$

where the experimental datum of the isoscalar mean square radius $\langle r^2 \rangle_{I=0}^{\text{exp}} \approx 0.806$ [fm].

Using (4.35), we calculate M_{KK} from the axial mean radius (4.46),

$$M_{\text{KK}} = \sqrt{\frac{3 \int_{-\infty}^\infty d\tilde{z} \tilde{k}(\tilde{z})^{-1} \int_0^{\tilde{z}} d\tilde{z}' \tilde{h}(\tilde{z}'; \zeta) \int_0^{\tilde{z}'} d\tilde{z}'' \tilde{k}(\tilde{z}''; \zeta)^{-1}}{\langle r^2 \rangle_A^{\text{exp}} \int_0^\infty d\tilde{z} \tilde{k}(\tilde{z})^{-1}}} =: \mathcal{B}_3(\zeta), \quad (4.57)$$

where the experimental datum of the axial mean square radius $\langle r^2 \rangle_A^{\text{exp}} \approx 0.674$ [fm].

The isoscalar magnetic moment (4.50) yields the relation

$$M_{\text{KK}} = \frac{\pi^4 (f_\pi^{\text{exp}})^2 g_{I=0}^{\text{exp}}}{M_N^{\text{exp}} \int_0^\infty d\tilde{z} \tilde{k}(\tilde{z}; \zeta)^{-1}} =: \mathcal{B}_4(\zeta). \quad (4.58)$$

The experimental data of the pion decay constant and the isoscalar magnetic moment are given by $f_\pi^{\text{exp}} \approx 92.4$ [MeV] and $g_{I=0}^{\text{exp}} \approx 1.76$. Substituting $N_c = 3$ into the isovector magnetic moment (4.52), M_{KK} is written down as

$$M_{\text{KK}} = \frac{2\sqrt{2}M_N^{\text{exp}}}{g_{I=1}^{\text{exp}}} \left(1 + 2\sqrt{\frac{14}{5}}\right) \frac{\zeta}{\sqrt{8\zeta^3 - 5}} =: \mathcal{B}_5(\zeta). \quad (4.59)$$

M_N^{exp} and $g_{I=1}^{\text{exp}}$ are given by the experimental values, $M_N^{\text{exp}} \approx 940$ [MeV] and $g_{I=1}^{\text{exp}} \approx 9.41$.

The meson spectra have been studied extensively in the literature. Here we consider the ρ and a_1 mesons. We match the calculated masses with the experimental data, so that

$$M_{\text{KK}} = \frac{m_\rho^{\text{exp}}}{m_\rho(\zeta)} =: \mathcal{M}_1(\zeta), \quad (4.60)$$

$$M_{\text{KK}} = \frac{m_{a_1}^{\text{exp}}}{m_{a_1}(\zeta)} =: \mathcal{M}_2(\zeta). \quad (4.61)$$

The functions $m_\rho(\zeta)$ and $m_{a_1}(\zeta)$ are dimensionless and have been evaluated numerically in [44]. The experimental values of the meson masses are described as $m_\rho^{\text{exp}} \approx 776$ [MeV] and $m_{a_1}^{\text{exp}} \approx 1230$ [MeV].

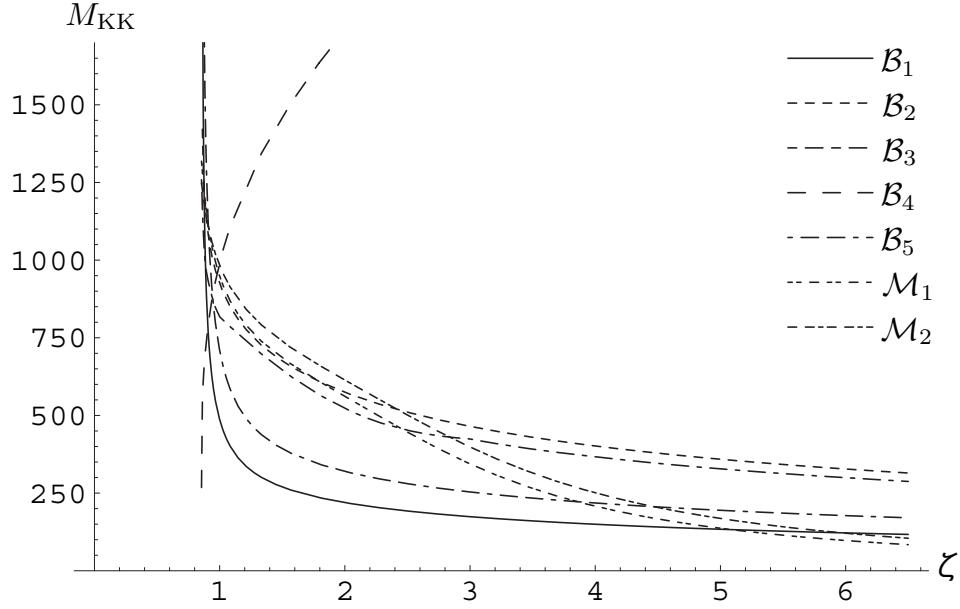


fig. 10 The behaviors of M_{KK} on ζ .

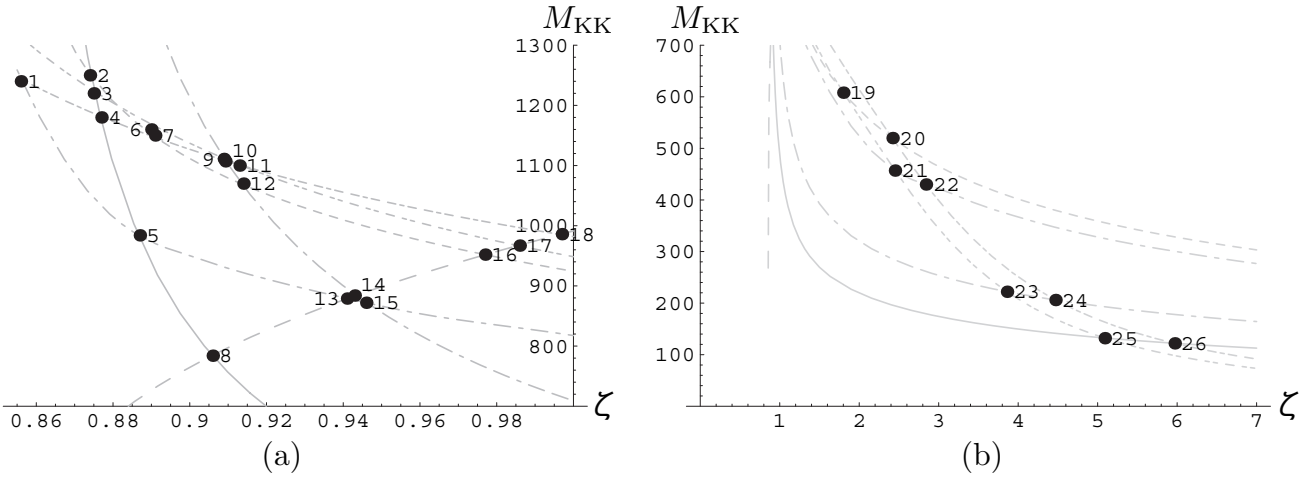


fig. 11 (a) The crossing points in $\zeta < 1$. (b) The crossing points in $\zeta \geq 1$.

The various forms of dependence of M_{KK} on ζ are depicted in fig. 10. In fig. 11 we enlarge the picture in the two regions where the various functions are crossing. One region (fig. 11 (a)) is in the “un-physical domain” where $\zeta < 1$, and the other is for $\zeta \geq 1$. The values (M_{KK}, ζ) of each crossing point in fig. 11 is listed in the following table:

| label | (ζ, M_{KK}) | label | (ζ, M_{KK}) | label | (ζ, M_{KK}) |
|-------|--------------------------|-------|--------------------------|-------|--------------------------|
| 1 | (0.856, 1240) | 10 | (0.909, 1110) | 19 | (1.80, 608) |
| 2 | (0.874, 1250) | 11 | (0.913, 1100) | 20 | (2.42, 520) |
| 3 | (0.875, 1220) | 12 | (0.914, 1070) | 21 | (2.45, 457) |
| 4 | (0.877, 1180) | 13 | (0.941, 879) | 22 | (2.84, 430) |
| 5 | (0.887, 984) | 14 | (0.943, 884) | 23 | (3.86, 222) |
| 6 | (0.890, 1160) | 15 | (0.946, 872) | 24 | (4.47, 206) |
| 7 | (0.891, 1150) | 16 | (0.977, 952) | 25 | (5.09, 132) |
| 8 | (0.906, 784) | 17 | (0.986, 967) | 26 | (5.97, 122) |
| 9 | (0.909, 1110) | 18 | (0.997, 986) | | |

Table 4: The crossing points in fig. 11.

(4.55) and (4.59) have no crossing point and $\mathcal{B}_5/\mathcal{B}_1$ is independent of ζ . $\mathcal{B}_5/\mathcal{B}_1$ should be equal to one in order for the prediction of the model to fit the observational values. In fact, substituting the experimental values, we evaluate

$$\mathcal{B}_5/\mathcal{B}_1 = \frac{(\sqrt{29} - \sqrt{14})(\sqrt{5} + 2\sqrt{14})g_{I=1}^{\text{exp}}}{1095M_N^{\text{exp}}} \approx 1.457,$$

which means 45.7% difference.

A better way to determine the values of the two parameters (ζ, M_{KK}) is by a fit of the calculated results to the experimental data using a χ^2 -method. This leads to the values

$$\zeta = 0.942, \quad M_{\text{KK}} = 997 \text{ [MeV]}. \quad (4.62)$$

Since in the model of [7] ζ must satisfy $\zeta \geq 1$ by definition, the result for ζ in (4.62) does not make sense. Let us ignore this problem for a moment, estimate the physical quantities naively by using the values (4.62) and then discuss possible scenario that yields this situation. The calculated results based on (4.62) are summarized in Table 5.

| | our model | experiment | discrepancy[%] |
|---------------------------------------|-----------|------------|----------------|
| m_ρ | 746 MeV | 776 MeV | -3.86 |
| m_{a_1} | 1160 MeV | 1230 MeV | -5.31 |
| $\frac{m_{\Delta(1232)}}{m_{n(940)}}$ | 1.51 | 1.31 | 15.2 |
| $\sqrt{\langle r^2 \rangle}_{I=0}$ | 0.813 fm | 0.806 fm | 0.920 |
| $\sqrt{\langle r^2 \rangle}_A$ | 0.594 fm | 0.674 fm | -11.9 |
| $g_{I=0}$ | 1.99 | 1.76 | 13.1 |
| $g_{I=1}$ | 8.41 | 9.41 | -10.7 |

Table 5: The χ^2 -fitting.

Note that, in Table 5, we fixed $m_{n(940)} = 940$ in the calculation of $m_{\Delta(1232)}/m_{n(940)}$. The axial coupling g_A is independent of M_{KK} , and is evaluated in terms of ζ in (4.62) as $g_A = 0.779$, which has -38.7% difference from the experimental value.

Now let us come back to the issue of possible meaning of (4.62). First notice that the value of ζ is larger than the critical value defined in Section 2, $\zeta_{cr} = (5/8)^{1/3}$. The fact that the value of ζ yielding the best fit came out to be in the un-physical region of $\zeta < 1$ may indicate that the description of the baryonic phenomena in the model [7], as given in [37], has to be modified. We cannot pinpoint the precise reason for that, but it might be that, due to local back reaction of the flavor brane with the baryon vertex on the background, the U-shaped cigar geometry is distorted so that effectively $\zeta < 1$ is allowed. Again we do not know that this is indeed the case but it seems to us that the fact that we have found the parameter ζ out of its region of definition may indicate a problem with the scenario for (4.62).

5. Baryons in single flavor model ($N_f = 1$)

We have started our journey with the baryon vertex attached to the flavor branes with N_c strings. In this picture, which was analyzed in Section 3, nothing forbids us from taking only one single flavor brane, namely $N_f = 1$. The heuristic arguments about the stability of the configuration apply also to the single flavor brane case, and moreover the conclusion that the baryon vertex is immersed in the flavor brane and does not hang out of it applies here as well. Thus, we conclude that there should be baryonic solutions for the abelian analog of (4.5) plus (4.10). In fact from the point of view of the underlying $SU(N_c)$ QCD theory, there is no reason that there will not exist baryonic states as singlets of the gauge symmetry composed from N_c quarks.

The action describing the theory on the single flavor, which is reduced from the expanded DBI action and the Chern-Simon term, takes the following form:

$$S_{N_f=1} = -\tilde{\kappa} \int d^4x d\tilde{z} \left(\frac{1}{2} \tilde{h}(\tilde{z}) F_{\mu\nu}^2 + \tilde{k}(\tilde{z}) F_{\mu\tilde{z}}^2 \right) + \frac{9\pi\kappa}{4\lambda} \int d^4x d\tilde{z} \epsilon^{ijk} A_0 F_{ij} F_{k\tilde{z}}. \quad (5.1)$$

Here $(A_\mu, A_{\tilde{z}})$ denotes a $U(1)$ gauge field in five dimensions.

The associated equations of motion are

$$\tilde{h}(\tilde{z}) \partial_i F^{i0} + \partial_{\tilde{z}}(\tilde{k}(\tilde{z}) F^{\tilde{z}0}) = -\frac{9\pi\kappa}{8\lambda\tilde{\kappa}} \epsilon^{ijk} F_{ij} F_{k\tilde{z}}, \quad (5.2a)$$

$$\tilde{h}(\tilde{z}) \partial_\mu F^{\mu i} + \partial_{\tilde{z}}(\tilde{k}(\tilde{z}) F^{\tilde{z}i}) = -\frac{9\pi\kappa}{8\lambda\tilde{\kappa}} \epsilon^{ijk} [2\partial_j(A_0 F_{k\tilde{z}}) + \partial_{\tilde{z}}(A_0 F_{jk})], \quad (5.2b)$$

$$\tilde{k}(\tilde{z}) \partial_\mu F^{\mu\tilde{z}} = \frac{9\pi\kappa}{8\lambda\tilde{\kappa}} \epsilon^{ijk} \partial_k(A_0 F_{ij}). \quad (5.2c)$$

For simplicity, we shall consider the anti-podal case ($\zeta = 1$), in which $\tilde{z} = z$, $\tilde{h}(\tilde{z}) = (1 + z^2)^{-1/3}$, $\tilde{k}(\tilde{z}) = 1 + z^2$ and $\tilde{\kappa} = \kappa$. We assume that the $U(1)$ gauge field is static and analyze the leading behavior in the λ^{-1} expansion under the rescaling (4.13). Then the equations of motion (5.2) are reduced to

$$\partial_M^2 A_0 = -\frac{9\pi}{8} \epsilon^{ijk} F_{ij} F_{kz}, \quad (5.3a)$$

$$\partial_M F^{MN} = 0. \quad (5.3b)$$

(5.3b) is the $U(1)$ version of the instanton equation in four-dimensional Euclidean space. Now it is well known that the abelian theory does not admit a non-singular instanton solution and thus we are facing a problem of how to identify the baryon in such a theory. In fact this situation is of no surprise, since in a similar manner there is no Skyrme solution to an abelian Skyrme-like theory.

We suspect that there should be a solution once we switch back the curvature nature of the five-dimensional model, namely when we include higher order corrections in $1/\lambda$. This is an open question that deserves a further study.

6. Baryons in six-dimensional holographic model

In analogy to SS model [7], one can introduce a stack of N_f D4-branes and a stack of N_f anti-D4-branes to the background of near extremal D4-branes of a six-dimensional non-critical gravity model [38,42]. The model, which like all other non-critical models suffers from the fact that it has order one curvature, is based on a compactified AdS_6 spacetime with a constant dilaton and hence does not suffer from large string coupling as happens in SS model. The spectra of mesons were analyzed in [45,46] and its thermal phase structure was determined in [47]. Most of the properties of the non-critical holographic model are similar to those of SS model, but some properties like the dependence of the meson masses on the stringy mass of the quarks and the excitation number are different.

The purpose of this section is to investigate the baryon configurations in the non-critical holographic model of [42] and to see how, if at all, it differs from those of the critical model. As was discussed in Section 3, the baryon vertex is a D4-brane wrapping the transverse S^4 cycle. In the six dimensional model by construction the S^4 does not exist, so one may wonder that the whole idea might not work for that model. However, one can use instead unwrapped D0-branes. In analogy to the Chern-Simon term on the

worldvolume of the wrapped D4-branes discussed in Section 3, there is also a Chern-Simon term of the form $N_c A_0 dt$ on the D0-brane worldvolume and hence also in this case one needs to attach N_c strings to the D0-baryon vertex. The other end of each of these strings will be obviously attached to the probe flavor D4-branes. Just as for the near extremal D4-branes of the critical model, and in fact as is shown in appendix A for any Dp branes, also in the non-critical model the baryon vertex will be attached to the probe branes. Let us now analyze the baryons in the corresponding five-dimensional theory.

The background of this model [38,42] is given by

$$\begin{aligned}
ds^2 &= \left(\frac{u}{R}\right)^2 [\eta_{\mu\nu} dx^\mu dx^\nu + f(u) dx_4^2] + \left(\frac{R}{u}\right)^2 \frac{du^2}{f(u)}, \\
e^\phi &= \frac{2\sqrt{2}}{\sqrt{3}N_c}, \quad F_{(6)} = -N_c \left(\frac{u}{R}\right)^4 dx_0 \wedge dx_1 \wedge dx_2 \wedge dx_3 \wedge dx_4 \wedge du, \\
R^2 &= \frac{15}{2}, \quad f(u) := 1 - \left(\frac{u_{\text{KK}}}{u}\right)^5.
\end{aligned} \tag{6.1}$$

Since the period of x_4 direction is $4\pi R^2/(5u_{\text{KK}})$, the mass scale is

$$M_{\text{KK}} = \frac{5u_{\text{KK}}}{2R^2}.$$

We concentrate on the $N_f = 2$ case and use the same decomposition of the $U(2)$ gauge field as in (4.9). In this background (6.1), the action of the flavor D4-branes is described by

$$\begin{aligned}
S &= T_4 \int d^5x e^{-\phi} \sqrt{-\det(g_{MN} + 2\pi\alpha' \mathcal{F}_{MN})} + T_4 \tilde{a} \int \mathcal{P}(C_{(5)}) + b \int \omega_5^{U(2)} \\
&= S_0 + S_{\text{YM}} + S_{\text{CS}} + \mathcal{O}(\mathcal{A}^3),
\end{aligned}$$

where

$$\begin{aligned}
S_0 &= T_4 e^{-\phi} \int d^4x dx_4 \left(\frac{u}{R}\right)^5 \left[\sqrt{f(u) + \left(\frac{R}{u}\right)^4 \frac{u'^2}{f(u)}} - a \right], \\
S_{\text{YM}} &= -\tilde{T} \int d^4x dz \text{tr} \left[\frac{1}{2} h(z) \eta^{\mu\nu} \eta^{\rho\sigma} F_{\mu\rho} F_{\nu\sigma} + M_{\text{KK}}^2 k(z) \eta^{\mu\nu} F_{\mu z} F_{\nu z} \right],
\end{aligned} \tag{6.2}$$

$$\begin{aligned}
S_{\text{CS}} &= b\epsilon^{MNPQ} \int d^4x dz \left[\frac{3}{8} \hat{A}_0 \text{tr}(F_{MN} F_{PQ}) - \frac{3}{2} \hat{A}_M \text{tr}(\partial_0 A_N F_{PQ}) \right. \\
&\quad \left. + \frac{3}{4} \hat{F}_{MN} \text{tr}(A_0 F_{PQ}) + \frac{1}{16} \hat{A}_0 \hat{F}_{MN} \hat{F}_{PQ} - \frac{1}{4} \hat{A}_M \hat{F}_{0N} \hat{F}_{PQ} \right],
\end{aligned} \tag{6.3}$$

up to total derivatives. \tilde{T} is equal to $(\pi\alpha')^2 T_4 R e^{-\phi} u_{\text{KK}}^{-1}$, which is proportional to N_c . So we describe $\tilde{T} := cN_c$. Note that \tilde{a}, b are constants and $a = (2/\sqrt{5})\tilde{a}$ [47]. Introducing the coordinate z defined by

$$\left(\frac{u}{u_{\text{KK}}}\right)^5 = \zeta^5 + \zeta^3 z^2, \quad \zeta := \frac{u_0}{u_{\text{KK}}},$$

we compute $h(z)$ and $k(z)$ in the power expansion for small z ,

$$\begin{aligned} h(z) &= h_0 + h_1 z^2 + \mathcal{O}(z^4), & k(z) &= k_0 + k_1 z^2 + \mathcal{O}(z^4), \\ h_0 &= \frac{4\zeta^{\frac{3}{2}}}{5\sqrt{2\zeta^5 - 1 - 2a\zeta^{5/2}\sqrt{\zeta^5 - 1}}}, & h_1 &= \frac{2(a^2 - 1)\zeta^{\frac{9}{2}}}{5\left(2\zeta^5 - 1 - 2a\zeta^{5/2}\sqrt{\zeta^5 - 1}\right)^{3/2}}, \\ k_0 &= \frac{4}{5}\zeta^{\frac{1}{2}}\sqrt{2\zeta^5 - 1 - 2a\zeta^{5/2}\sqrt{\zeta^5 - 1}}, & k_1 &= \frac{2}{25}\frac{(13 - 5a^2)\zeta^5 - 4 - 8a\zeta^{5/2}\sqrt{\zeta^5 - 1}}{\zeta^{3/2}\sqrt{2\zeta^5 - 1 - 2a\zeta^{5/2}\sqrt{\zeta^5 - 1}}}. \end{aligned}$$

Without any loss of generality, we can set $M_{\text{KK}} = 1$ again. Using the rescaling

$$\begin{aligned} x^0 &\rightarrow x^0, & x^i &\rightarrow \frac{1}{\sqrt{N_c}}x^i, & z &\rightarrow \frac{1}{\sqrt{N_c}}z, \\ \mathcal{A}_0 &\rightarrow \mathcal{A}_0, & \mathcal{A}_i &\rightarrow \sqrt{N_c}\mathcal{A}_i, & \mathcal{A}_z &\rightarrow \sqrt{N_c}\mathcal{A}_z, \end{aligned} \tag{6.4}$$

the Yang-Mills action (6.2) is expanded with respect to the large N_c ,

$$\begin{aligned} S_{\text{YM}} &= -c \int d^4x dz \text{tr} \left[N_c \left(\frac{1}{2} h_0 F_{ij}^2 + k_0 F_{iz}^2 \right) \right. \\ &\quad \left. + \frac{1}{2} h_1 z^2 F_{ij}^2 + k_1 z^2 F_{iz}^2 - h_0 F_{0i}^2 - k_0 F_{0z}^2 + \mathcal{O}(N_c^{-1}) \right] \\ &\quad - c \int d^4x dz \frac{1}{2} \left[N_c \left(\frac{1}{2} h_0 \hat{F}_{ij}^2 + k_0 \hat{F}_{iz}^2 \right) \right. \\ &\quad \left. + \frac{1}{2} h_1 z^2 \hat{F}_{ij}^2 + k_1 z^2 \hat{F}_{iz}^2 - h_0 \hat{F}_{0i}^2 - k_0 \hat{F}_{0z}^2 + \mathcal{O}(N_c^{-1}) \right]. \end{aligned}$$

Then the equations of motion for the $SU(2)$ part are described as

$$h_0 D^i F_{i0} + k_0 D^z F_{z0} - \frac{3b}{8c} \epsilon^{MNPQ} \hat{F}_{MN} F_{PQ} = 0, \tag{6.5a}$$

$$h_0 D^i F_{ij} + k_0 D^z F_{zj} = 0, \tag{6.5b}$$

$$k_0 D^i F_{iz} = 0, \tag{6.5c}$$

while the equations of motion for the $U(1)$ part are

$$h_0 \partial^i \hat{F}_{i0} + k_0 \partial^z \hat{F}_{z0} - \frac{3b}{8c} \epsilon^{MNPQ} \left[\text{tr}(F_{MN} F_{PQ}) + \frac{1}{2} \hat{F}_{MN} \hat{F}_{PQ} \right] = 0, \quad (6.6a)$$

$$h_0 \partial^i \hat{F}_{ij} + k_0 \partial^z \hat{F}_{zj} = 0, \quad (6.6b)$$

$$k_0 \partial^i \hat{F}_{iz} = 0. \quad (6.6c)$$

Since (6.5b, c) correspond to the instanton equation, in completely the same way as in SS model, the equations of motion (6.5) and (6.6) can be solved as

$$A_M(x^i, z) = -iv(\xi)g\partial_M g^{-1} \quad (M = 1, 2, 3, z), \quad (6.7a)$$

$$A_0 = 0, \quad (6.7b)$$

$$\hat{A}_M = 0, \quad (6.7c)$$

$$\hat{A}_0 = \frac{3b}{c\sqrt{h_0 k_0}} \frac{1}{\xi^2} \left[1 - \frac{\rho^4}{(\xi^2 + \rho^2)^2} \right], \quad (6.7d)$$

where

$$v(\xi) = \frac{\xi^2}{\xi^2 + \rho^2}, \quad g(x^i, z) = \frac{s(z - Z)\mathbf{1} - i(x^i - X^i)\tau_i}{\xi},$$

$$\xi := \sqrt{(x^i - X^i)^2 + s^2(z - Z)^2}, \quad s := \sqrt{\frac{h_0}{k_0}}.$$

These solutions (6.7) lead to the baryon mass,

$$\begin{aligned} M &= N_c c \int d^3 x dz \text{tr} \left(\frac{h_0}{2} F_{ij}^2 + k_0 F_{iz}^2 \right) \\ &+ c \int d^3 x dz \left[\text{tr} \left(\frac{h_1}{2} z^2 F_{ij}^2 + k_1 z^2 F_{iz}^2 \right) - \frac{h_0}{2} (\partial_i \hat{A}_0)^2 - \frac{k_0}{2} (\partial_z \hat{A}_0)^2 \right. \\ &\quad \left. - \frac{3b}{8c} \epsilon^{MNPQ} \hat{A}_0 \text{tr}(F_{MN} F_{PQ}) \right] + \mathcal{O}(N_c^{-1}) \\ &= \frac{32\pi^2 c}{5} N_c \zeta + \frac{32\pi^2 c}{25\zeta} Y^2 \\ &+ \frac{16\pi^2 c}{25\zeta^2} \left(2\zeta^5 - 1 - 2a\zeta^{5/2} \sqrt{\zeta^5 - 1} \right) \rho^2 + \frac{18\pi^2 b^2}{\zeta} \frac{1}{\rho^2} + \mathcal{O}(N_c^{-1}). \end{aligned}$$

The critical value of Y and ρ minimizing the baryon mass M is evaluated

$$Y_{\text{cr}} = 0, \quad \rho_{\text{cr}}^2 = \frac{15b}{2\sqrt{2}c} \sqrt{\frac{\zeta}{2\zeta^5 - 1 - 2a\zeta^{5/2} \sqrt{\zeta^5 - 1}}}.$$

Since the non-critical model has an effective 't Hooft model of order one, we find that in the non-critical case the size of the baryon is order one.

7. Conclusions and discussions

We have considered the baryon sector in the non-anti-podal SS model, where the parameter ζ is introduced in addition to Kaluza-Klein mass M_{KK} and 't Hooft coupling λ . This model converges to the original (anti-podal) SS model at $\zeta = 1$.

The baryon mass formula (4.25) has been calculated as a function of ζ and M_{KK} . We have compared the mass spectra with the experiment in the two ways. Firstly, identifying the two lowest modes with the experimental values of $n(940)$ and $\Delta(1232)$, we have obtained the relation (4.30) between ζ and M_{KK} and computed the mass spectra of N and Δ baryons as shown in Table 2. The relation (4.30) implies that M_{KK} is bounded to be less than 487 MeV because of $\zeta \geq 1$ by definition. Secondly the baryon masses have been evaluated by the use of the minimal χ^2 fitting. In this method, we can read that the upper bound of M_{KK} is 424.8 MeV. Anyway, in both cases, M_{KK} does not reach 949 MeV used in [7,37].

By following the method given by [37], we have analyzed the isoscalar, isovector and axial mean square radii, the isoscalar and isovector magnetic moments and the axial coupling. We have incorporated these physical quantities with the mass spectra of the baryons and ρ and a_1 mesons, and compared them with the experiment. Then we have obtained M_{KK} as the functions of ζ , which are depicted in fig. 10. From these analyses we conclude that the $\zeta = 1$ model, that is, the original SS model, is fitted best to the experiment. However, if without any justification $\zeta < 1$ is permitted by some modification of SS model, we have found that the best-fitted values of (ζ, M_{KK}) are $(0.942, 997[\text{MeV}])$ by the use of the χ^2 method. The physical quantities computed with these values are listed in Table 5 and are in good agreement with the experiment. Though the appropriate modification of the incorporation of baryons to SS model is still not clear to us, here there are two possible options:

- Since the weighted baryon vertex which is located at the tip of the U-shaped flavor D8-branes has an object with energy that scales with N_c , it might backreact on the flavor brane and also on the background geometry in such a way that the tip of the cigar would be pulled down to $u_{\text{KK}}^* (< u_{\text{KK}})$. Then ζ , which defined by (4.1), can take the value in $\zeta \geq u_{\text{KK}}^*/u_{\text{KK}}$, where the lower bound of ζ is smaller than one.
- SS model is the dual of massless QCD. In order to put mass on the quarks, we need to consider the contribution of the open strings ending on the flavor D8-branes [33–36]. The tension of the open strings would pull up the D8-branes and the best-fitted value of ζ , which is smaller than one, might be recovered to the value in $\zeta \geq 1$.

We have also calculated the energy of the D4-brane wrapped in S^4 as a baryon vertex and analyzed its stability with respect to the location u_B on the u direction. In the confinement phase, the energy is monotonic on u_B , the baryon vertex is stabilized at $u_B = u_0$, that is to say, the baryon vertex stays at the tip of the flavor D8-branes. On the other hand, in the deconfinement phase, there appears an interesting property. This is caused by the balance between the tension of the N_c open strings, which corresponds to the quarks of baryon, and the attractive force from the black hole. The parameter u_T corresponds to temperature. Here we consider the behavior of the baryon vertex with respect to u_T by fixing the tip of the D8-branes u_0 . If $x_0(= u_0/u_T)$ is larger than x_{cr} given by (3.1), the baryon vertex becomes stable at the tip of the D8-branes. If x_0 is smaller than x_{cr} , the baryon vertex goes to the tip of the cigar background, which is a black hole. In other words, the baryon vertex can be realized at the tip of the D8-branes at temperatures lower than a critical temperature, but it falls down into the black hole at temperatures higher than the critical temperature. This property is similar to the chiral symmetry restoration [30].

Finally we have commented on the single flavor model. It is impossible to apply the Skyrme model to the case of single flavor, because there does not exist a $U(1)$ instanton. On the other hand, in the holographic models, we can easily suppose the picture of the baryon vertex with single flavor. Though the instanton solution also plays an important role in our analysis of baryons, we conclude that the singular solution of the $U(1)$ gauge field is interpreted as the baryon.

Acknowledgments

We would like to thank Ofer Aharony and Vadim Kaplunovsky for useful conversations and their comments on the manuscript. JS would like to thank Elias Kiritsis and Shigeki Sugimoto for fruitful discussion during the Institute d'ete, Ecole Normal. This work was supported in part by a center of excellence supported by the Israel Science Foundation (grant number 1468/06), by a grant (DIP H52) of the German Israel Project Cooperation, by a BSF United States-Israel binational science foundation grant 2006157 and by the European Network MRTN-CT-2004-512194. The work of JS was also supported in part by European Union Excellence Grant MEXT-CT-2003-509661. SS are grateful to Institute of Physical and Chemical Research (RIKEN) and Yukawa Institute for Theoretical Physics (YITP) for their hospitality. Part of the work was done while SS was visiting YITP with

partial support by the Grant-in-Aid for the Global COE Program “The Next Generation of Physics, Spun from Universality and Emergence” from the Ministry of Education, Culture, Sports, Science and Technology (MEXT) of Japan.

Appendix A. baryon vertex in Dp-branes’ background

Let us consider the energy E_p of D(8-p)-brane wrapped on S^{8-p} and N_c fundamental strings, which is denoted by

$$S_p = -T_{8-p} \int dt d\Omega_{8-p} e^{-\phi} \sqrt{-\det g_{D(8-p)}} - N_c T_f \int dt du \sqrt{-\det g_{\text{string}}} =: \int dt E_p,$$

where the tension of D(8-p)-brane $T_{8-p} = (2\pi)^{p-8} l_s^{p-9}$.

A.1. Confinement phase

The metric of the background is described as

$$ds^2 = \left(\frac{u}{R_p}\right)^{\frac{7-p}{2}} \left[-dt^2 + \sum_{i=1}^{p-1} (dx^i)^2 + f(u; p) (dx^p)^2 \right] + \left(\frac{R_p}{u}\right)^{\frac{7-p}{2}} \left[\frac{du^2}{f(u; p)} + u^2 d\Omega_{8-p} \right],$$

$$R_p^{7-p} = \frac{g_s N_c (2\pi l_s)^{7-p}}{(7-p) V_{8-p}}, \quad e^\phi = g_s \left(\frac{R_p}{u}\right)^{\frac{(7-p)(3-p)}{4}}, \quad f(u; p) = 1 - \left(\frac{u_\Lambda}{u}\right)^{7-p},$$

where V_{8-p} is the unit volume of S^{8-p} , which is equal to $2\pi^{(9-p)/2} / \Gamma((9-p)/2)$. The energy is described as

$$E_p(u_B; u_0) = \frac{N_c u_\Lambda}{2\pi l_s^2} \mathcal{E}_{\text{conf}}^{(p)}, \quad \mathcal{E}_{\text{conf}}^{(p)}(x; x_0) = \frac{1}{7-p} x + \int_x^{x_0} \frac{dy}{\sqrt{1-y^{p-7}}},$$

$$x := \frac{u_B}{u_\Lambda}, \quad x_0 := \frac{u_0}{u_\Lambda}, \quad 1 \leq x \leq x_0.$$

The integration can be computed in terms of the hypergeometric function ${}_2F_1$,

$$\int_x^{x_0} \frac{dy}{\sqrt{1-y^{p-7}}} = -\frac{2ix^{\frac{9-p}{2}}}{9-p} {}_2F_1\left(\frac{p-9}{2p-14}, \frac{1}{2}, \frac{23-3p}{14-2p}, x^{7-p}\right)$$

$$+ \frac{2ix_0^{\frac{9-p}{2}}}{9-p} {}_2F_1\left(\frac{p-9}{2p-14}, \frac{1}{2}, \frac{23-3p}{14-2p}, x_0^{7-p}\right).$$

A.2. Deconfinement phase

The metric of the background is described as

$$ds^2 = \left(\frac{u}{R_p}\right)^{\frac{7-p}{2}} \left[-f_T(u; p) dt^2 + \sum_{i=1}^p (dx^i)^2 \right] + \left(\frac{R_p}{u}\right)^{\frac{7-p}{2}} \left[\frac{du^2}{f_T(u; p)} + u^2 d\Omega_{8-p} \right],$$

$$R_p^{7-p} = \frac{g_s N_c (2\pi l_s)^{7-p}}{(7-p)V_{8-p}}, \quad e^\phi = g_s \left(\frac{R_p}{u}\right)^{\frac{(7-p)(3-p)}{4}}, \quad f_T(u; p) = 1 - \left(\frac{u_T}{u}\right)^{7-p}.$$

The energy E_p can be evaluated,

$$E_p(u_B; u_0) = \frac{N_c u_T}{2\pi l_s^2} \mathcal{E}_{\text{deconf}}^{(p)}, \quad \mathcal{E}_{\text{deconf}}^{(p)}(x; x_0) = \frac{1}{7-p} x \sqrt{1-x^{p-7}} + (x_0 - x),$$

$$x := \frac{u_B}{u_T}, \quad x_0 := \frac{u_0}{u_T}, \quad 1 \leq x \leq x_0.$$

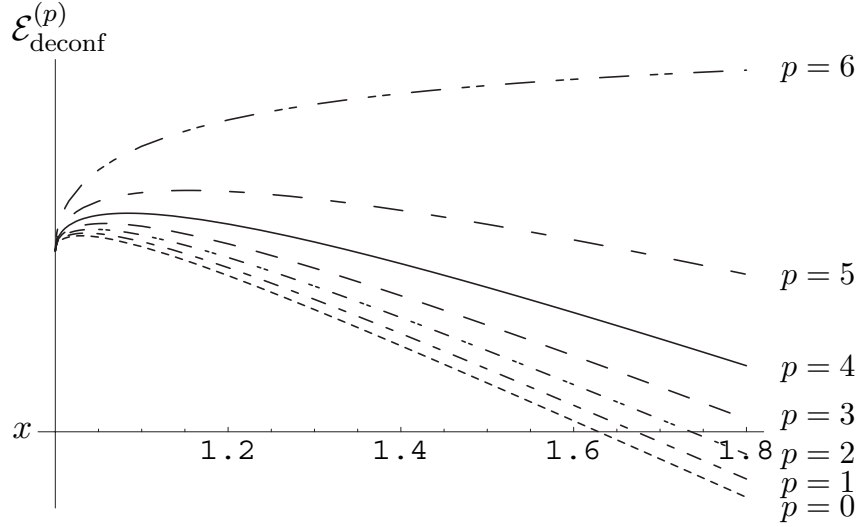


fig. 12 $\mathcal{E}_{\text{deconf}}^{(p)}(x)$

Fig. 12 implies that only $E_6(u_B)$ is a monotonically increasing function.

References

- [1] E. Witten, “Baryons and Branes in Anti de Sitter Space,” *JHEP* **9807** (1998) 006 [arXiv:hep-th/9805112].
- [2] D. J. Gross and H. Ooguri, “Aspects of Large N Gauge Theory Dynamics as Seen by String Theory,” *Phys. Rev. D* **58** (1998) 106002 [arXiv:hep-th/9805129].
- [3] Y. Imamura, “String Junctions and Their Duals in Heterotic String Theory,” *Prog. Theor. Phys.* **101** (1999) 1155 [arXiv:hep-th/9901001].
- [4] C. G. Callan, A. Guijosa and K. G. Savvidy, “Baryons and String Creation from the Fivebrane Worldvolume Action,” *Nucl. Phys. B* **547** (1999) 127 [arXiv:hep-th/9810092].
- [5] C. G. Callan, A. Guijosa, K. G. Savvidy and O. Tafjord, “Baryons and Flux Tubes in Confining Gauge Theories from Brane Actions,” *Nucl. Phys. B* **555** (1999) 183 [arXiv:hep-th/9902197].
- [6] A. Brandhuber, N. Itzhaki, J. Sonnenschein and S. Yankielowicz, “Baryons from Supergravity,” *JHEP* **9807** (1998) 020 [arXiv:hep-th/9806158].
- [7] T. Sakai and S. Sugimoto, “Low Energy Hadron Physics in Holographic QCD,” *Prog. Theor. Phys.* **113** (2005) 843 [arXiv:hep-th/0412141].
- [8] E. Witten, “Anti-de Sitter Space, Thermal Phase Transition, and Confinement in Gauge Theories,” *Adv. Theor. Math. Phys.* **2** (1998) 505 [arXiv:hep-th/9803131].
- [9] H. Hata, T. Sakai, S. Sugimoto and S. Yamato, “Baryons from Instantons in Holographic QCD,” arXiv:hep-th/0701280.
- [10] D. K. Hong, M. Rho, H. U. Yee and P. Yi, “Chiral Dynamics of Baryons from String Theory,” *Phys. Rev. D* **76** (2007) 061901 [arXiv:hep-th/0701276].
- [11] A. Imaanpur, “On Instantons in Holographic QCD,” arXiv:0705.0496 [hep-th].
- [12] D. K. Hong, M. Rho, H. U. Yee and P. Yi, “Dynamics of Baryons from String Theory and Vector Dominance,” *JHEP* **0709** (2007) 063 [arXiv:0705.2632 [hep-th]].
- [13] O. Bergman, G. Lifschytz and M. Lippert, “Holographic Nuclear Physics,” *JHEP* **0711** (2007) 056 [arXiv:0708.0326 [hep-th]].
- [14] M. Rozali, H. H. Shieh, M. Van Raamsdonk and J. Wu, “Cold Nuclear Matter in Holographic QCD,” *JHEP* **0801** (2008) 053 [arXiv:0708.1322 [hep-th]].
- [15] K. Y. Kim, S. J. Sin and I. Zahed, “The Chiral Model of Sakai-Sugimoto at Finite Baryon Density,” *JHEP* **0801** (2008) 002 [arXiv:0708.1469 [hep-th]].
- [16] H. Hata and M. Murata, “Baryons and the Chern-Simons Term in Holographic QCD with Three Flavors,” *Prog. Theor. Phys.* **119** (2008) 461 [arXiv:0710.2579 [hep-th]].
- [17] K. Y. Kim, S. J. Sin and I. Zahed, “Dense Holographic QCD in the Wigner-Seitz Approximation,” *JHEP* **0809** (2008) 001 [arXiv:0712.1582 [hep-th]].
- [18] Y. Seo and S. J. Sin, “Baryon Mass in Medium with Holographic QCD,” *JHEP* **0804** (2008) 010 [arXiv:0802.0568 [hep-th]].

- [19] H. Hata, M. Murata and S. Yamato, “Chiral Currents and Static Properties of Nucleons in Holographic QCD,” arXiv:0803.0180 [hep-th].
- [20] K. Y. Kim, S. J. Sin and I. Zahed, “Dense and Hot Holographic QCD: Finite Baryonic E Field,” JHEP **0807** (2008) 096 [arXiv:0803.0318 [hep-th]].
- [21] D. K. Hong, K. M. Lee, C. Park and H. U. Yee, “Holographic Monopole Catalysis of Baryon Decay,” JHEP **0808** (2008) 018 [arXiv:0804.1326 [hep-th]].
- [22] J. Park and P. Yi, “A Holographic QCD and Excited Baryons from String Theory,” JHEP **0806** (2008) 011 [arXiv:0804.2926 [hep-th]].
- [23] O. Bergman, G. Lifschytz and M. Lippert, “Magnetic Properties of Dense Holographic QCD,” arXiv:0806.0366 [hep-th].
- [24] K. Y. Kim and I. Zahed, “Electromagnetic Baryon Form Factors from Holographic QCD,” JHEP **0809** (2008) 007 [arXiv:0807.0033 [hep-th]].
- [25] K. Hashimoto, “Holographic Nuclei,” arXiv:0809.3141 [hep-th].
- [26] K. Nawa, H. Suganuma and T. Kojo, “Baryons in Holographic QCD,” Phys. Rev. D **75** (2007) 086003 [arXiv:hep-th/0612187];
- [27] K. Nawa, H. Suganuma and T. Kojo, “Brane-induced Skyrmion on S^3 : baryonic matter in holographic QCD,” arXiv:0810.1005 [hep-th].
- [28] G. S. Adkins and C. R. Nappi, “The Skyrme Model with Pion Masses,” Nucl. Phys. B **233** (1984) 109.
- [29] A. Pomarol and A. Wulzer, “Baryon Physics in Holographic QCD,” arXiv:0807.0316 [hep-ph].
- [30] O. Aharony, J. Sonnenschein and S. Yankielowicz, “A Holographic Model of Deconfinement and Chiral Symmetry Restoration,” Annals Phys. **322** (2007) 1420 [arXiv:hep-th/0604161].
- [31] M. Kruczenski, L. A. P. Zayas, J. Sonnenschein and D. Vaman, “Regge Trajectories for Mesons in the Holographic Dual of Large- N_c QCD,” JHEP **0506** (2005) 046 [arXiv:hep-th/0410035].
- [32] R. Casero, E. Kiritsis and A. Paredes, “Chiral Symmetry Breaking as Open String Tachyon Condensation,” Nucl. Phys. B **787** (2007) 98 [arXiv:hep-th/0702155].
- [33] O. Bergman, S. Seki and J. Sonnenschein, “Quark Mass and Condensate in HQCD,” JHEP **0712** (2007) 037 [arXiv:0708.2839 [hep-th]].
- [34] A. Dhar and P. Nag, “Sakai-Sugimoto Model, Tachyon Condensation and Chiral Symmetry Breaking,” JHEP **0801** (2008) 055 [arXiv:0708.3233 [hep-th]].
- [35] O. Aharony and D. Kutasov, “Holographic Duals of Long Open Strings,” arXiv:0803.3547 [hep-th].
- [36] K. Hashimoto, T. Hirayama, F. L. Lin and H. U. Yee, “Quark Mass Deformation of Holographic Massless QCD,” JHEP **0807** (2008) 089 [arXiv:0803.4192 [hep-th]].
- [37] K. Hashimoto, T. Sakai and S. Sugimoto, “Holographic Baryons : Static Properties and Form Factors from Gauge/String Duality,” arXiv:0806.3122 [hep-th].

- [38] S. Kuperstein and J. Sonnenschein, “Non-critical, Near Extremal AdS_6 Background as a Holographic Laboratory of Four Dimensional YM Theory,” *JHEP* **0411** (2004) 026 [arXiv:hep-th/0411009].
- [39] T. Sakai and S. Sugimoto, “More on a Holographic Dual of QCD,” *Prog. Theor. Phys.* **114** (2006) 1083 [arXiv:hep-th/0507073].
- [40] C. G. Callan and J. M. Maldacena, “Brane Dynamics from the Born-Infeld Action,” *Nucl. Phys. B* **513** (1998) 198 [arXiv:hep-th/9708147].
- [41] A. A. Belavin, A. M. Polyakov, A. S. Shvarts and Yu. S. Tyupkin, “Pseudoparticle Solutions of the Yang-Mills Equations,” *Phys. Lett. B* **59** (1975) 85.
- [42] S. Kuperstein and J. Sonnenschein, “Non-critical Supergravity ($d > 1$) and Holography,” *JHEP* **0407** (2004) 049 [arXiv:hep-th/0403254].
- [43] W. M. Yao *et al.* [Particle Data Group], “Review of Particle Physics,” *J. Phys. G* **33** (2006) 1.
- [44] K. Peeters and M. Zamaklar, private communication.
- [45] R. Casero, A. Paredes and J. Sonnenschein, “Fundamental Matter, Meson Spectroscopy and Non-critical String / Gauge Duality,” *JHEP* **0601** (2006) 127 [arXiv:hep-th/0510110].
- [46] O. Mintkevich and N. Barnea, “Wave Function for No-core Effective Interaction Approaches,” *Phys. Rev. C* **69** (2004) 044005.
- [47] V. Mazo and J. Sonnenschein, “Non Critical Holographic Models of the Thermal Phases of QCD,” *JHEP* **0806** (2008) 091 [arXiv:0711.4273 [hep-th]].